Unconventional photon blockade with non-Markovian effects in driven dissipative coupled cavities

H. Z. Shen [1,2,*] J. F. Yang,[1] and X. X. Yi[1,2,†]

[1] *Center for Quantum Sciences and School of Physics, Northeast Normal University, Changchun 130024, China*

[2] *Center for Advanced Optoelectronic Functional Materials Research, and Key Laboratory for UV Light-Emitting Materials and Technology of Ministry of Education, Northeast Normal University, Changchun 130024, China*

(Received 11 September 2023; revised 21 February 2024; accepted 8 April 2024; published 29 April 2024)

The photon blockade based on destructive quantum interference is called the unconventional photon blockade (UPB), which has been intensively studied in Markovian systems but barely explored in the non-Markovian ones. In this paper, we construct a coupled-cavities system to achieve UPB with the non-Markovian effect, where the dissipationless left cavity and Markovian dissipative right cavity are respectively mediated by two-photon pump and single-photon driving field. Through the equivalence between the Markovian master equation and Heisenberg-Langevin equation for the environment initialization in the vacuum state, we can derive the exact non-Markovian Heisenberg-Langevin equation and reduced master equation for the left cavity, which contains the two-photon pump and effective single-photon driving field. In the non-Markovian regime (the dissipation falling below a threshold), the effective single-photon driving field holds nonzero, which can lead to UPB occurring due to a closed quantum interference path forming. When the dissipation exceeds the threshold, the system enters the Markovian regime, where UPB weakens. Especially, if the dissipation approaches infinity, UPB for the left cavity disappears due to the effective single-photon driving field tending to zero. We analytically derive an optimal condition for UPB, which is in good agreement with that obtained by the numerical simulation. We also discuss the situation where both cavities have dissipations. Finally, the above model is extended to a general system involving a dissipationless left cavity (mediated by two-photon pump) coupling with noninteracting dissipative right cavities (driven by single-photon driving fields). Our scheme might pave an avenue towards applications on photon statistics and quantum optics with the non-Markovian effect.

DOI: 10.1103/PhysRevA.109.043714

I. INTRODUCTION

The photon blockade [1] originates from the anharmonic dynamics of bosonic modes and has been used for generating optical fields with nonclassical statistics [2,3] and single-photon sources [4,5], which is known as the conventional photon blockade (CPB) with large nonlinearities with respect to the decay rate of the system. The CPB was first observed in an optical cavity coupled to a single trapped atom [6]. Subsequently, strong antibunching behaviors were obtained in different systems by a series of research groups, including a quantum dot in a photonic crystal system [7], circuit cavity quantum electrodynamics systems [8–19], and circuit QED [20,21]. The theoretical models about CPB include quantum optomechanical systems [22–35], exciting polaritons [36], two-level systems coupled to the cavity [37–44], dynamical blockade [45], quantum dots coupled to a nanophotonic waveguide [46], four-level quantum emitters [47], and three-wave mixing [48]. Many schemes have been completed in nanostructured cavities and semiconductor microcavities with second-order [49–52] and three-order nonlinearities [53,54]. The potential applications of photon blockade include the realization of interferometers [55], quantum nonreciprocity [56,57], single-photon transistors [58], non-Hermitian photon blockade [59–68], nonreciprocal CPB [69–75], and multiphoton blockade [76–87].

Unconventional photon blockade (UPB) [88] with nonlinearities weaker than the decay rates of the cavity modes has been proposed to suppress the multiphoton population by utilizing the quantum interference between different paths of transitions [89–94]. Such a scheme requires an additional degree of freedom of photons, such as an ancillary photonic mode or emitter to provide an extra dimension for the construction of different transition pathways. With the fundamental principle, many quantum systems are predicted to have photon blockade effect with weak nonlinearities, such as bimodal coupled polaritonic cavities [95], optical cavities with a quantum dot [96–103], coupled single-mode cavities with second- or third-order nonlinearity [104–113], three-level artificial atoms [114,115], optomechanical systems [116–118], semiconductor cavities [119], Gaussian squeezed states [120–122], and nonreciprocal UPB [123–131]. Moreover, UPB in the microwave domain has been observed in coupled superconducting resonators [132] and quantum dot cavity QED [133] in experiment.

In general, all the quantum systems in reality are open owing to the unavoidable coupling with the environments [134–144], which have attracted more and more attention with

*Corresponding author: shenhz458@nenu.edu.cn

†Corresponding author: yixx@nenu.edu.cn

the rapid development of quantum information technology [145,146]. The Markovian approximation for open systems [136,144] is only valid when the coupling between the system and environment is weak and characteristic time of the system under study is adequately larger than that of the environment. Otherwise we need to investigate the influences of the non-Markovian environment on the system dynamics [147–149], which occurs in many quantum systems including coupled cavities [150], photonic crystals [151,152], colored noises [153], cavities coupled to waveguides [154–157], and implementations in experiment [158–174]. The non-Markovian process proves to be useful in quantum information processing including quantum state engineering, quantum control, and quantum channel capacity [175,176]. With the different measures of non-Markovianities [177–184], the non-Markovian effects of the environments backacting on the system can be characterized by the excitation backflow between the system and its environment [185–190].

The above considerations motivate us to explore the following questions.

(i) How do we achieve UPB in the non-Markovian regime?

(ii) Under what condition will UPB disappear?

For this purpose, we propose a coupled-cavities scheme to realize UPB with the non-Markovian effect, where the two-photon pump and single-photon driving field respectively drive the dissipationless left cavity and Markovian dissipative right cavity. We derive the exact non-Markovian Heisenberg-Langevin equation and reduced master equation for the left cavity, which are mediated by two-photon pump and effective single-photon driving field. We analytically derive the optimal condition for UPB in the non-Markovian regime when the dissipation falls below a threshold, which coincides well with the numerical simulation by solving the master equation. The dissipation greater than the threshold corresponds to the Markovian regime, which can weaken UPB. Especially, UPB disappears for the left cavity due to the closed quantum interference paths being broken when the dissipation reaches infinity. The situation of both cavities having dissipations is also discussed. Finally, we extend the model to the general system involving a two-photon pumped left cavity coupling with noninteracting single-photon driven dissipative right cavities.

The remainder of the paper is organized as follows. In Sec. II, we introduce a model to describe the system under study consisting of the dissipationless left cavity and Markovian dissipative right cavity respectively mediated by two-photon pump and single-photon driving field. The optimal condition for UPB is derived. In Sec. III, we give the exact reduced non-Markovian Heisenberg-Langevin equation for the left cavity. In Sec. IV, the exact non-Markovian master equation for the left cavity is derived. In Sec. IV, we discuss UPB with the non-Markovian effect under the optimal condition. In Sec. V, we analytically derive the second-order correlation function and compare it with that derived by the numerical simulation. In Sec. VI, we discuss the situation where both cavities have dissipations. In Sec. VII, a two-photon pumped left cavity coupling with noninteracting single-photon driven dissipative right cavities is presented. Section VIII is devoted to conclusions.

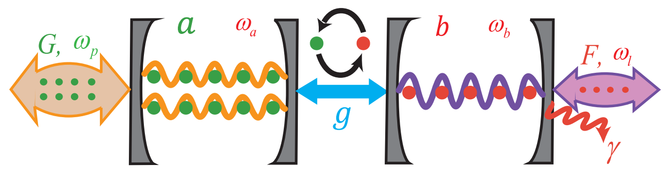

FIG. 1. Setup for UPB with the non-Markovian effect. The left cavity (eigenfrequency ω_a) and right cavity (eigenfrequency ω_b) with the coupling strength g are mediated by the two-photon pump (strength G and frequency ω_p) [13,90,120–122,191–198] and single-photon driving field (strength F and frequency ω_l), respectively. The left cavity is assumed to have no photon leakage (also see discussions for the dissipation to the left cavity in Sec. VI), while the right cavity has the dissipation γ with the Markovian approximation.

II. MODEL AND UPB

A. Markovian master equation for the system

To present the model to realize UPB with the non-Markovian effect, we consider that the system under study is composed of two coupled cavities outlined in Fig. 1, where the left cavity (cavity a) is mediated by two-photon pump [199,200], while the right cavity (cavity b) is driven by single-photon driving field. The Hamiltonian reads ($\hbar \equiv 1$)

$$\hat{H}_0 = \omega_a\hat{a}^\dagger\hat{a} + \omega_b\hat{b}^\dagger\hat{b} + G(\hat{a}^{\dagger 2}e^{-i\omega_p t-2i\theta} + \hat{a}^2 e^{i\omega_p t+2i\theta}) + g(\hat{a}\hat{b}^\dagger + \hat{a}^\dagger\hat{b}) + F^*\hat{b}e^{i\omega_l t} + F\hat{b}^\dagger e^{-i\omega_l t}, \tag{1}$$

where the first and second terms on the right-hand side describe the free Hamiltonian of the left cavity at eigenfrequency ω_a and right cavity at eigenfrequency ω_b with annihilation (creation) operators $\hat{a}$ ($\hat{a}^\dagger$) and $\hat{b}$ ($\hat{b}^\dagger$) satisfying the Bosonic commutation relations $[\hat{a}, \hat{a}^\dagger] = 1$ and $[\hat{b}, \hat{b}^\dagger] = 1$, respectively. The third term denotes the two-photon pump to the left cavity with frequency ω_p and conversion rate G, whose possible realization can be found in Appendix A. The fourth term corresponds to the tunneling coupling between two cavities with the coupling strength g. The last two terms denote the single-photon driving field to the right cavity with amplitude $F = fe^{-i\phi}$ (strength f and phase ϕ) and frequency ω_l. In a rotating frame defined by $U(t) = \exp[-i\omega_l t(\hat{a}^\dagger\hat{a} + \hat{b}^\dagger\hat{b})]$ with $\omega_p = 2\omega_l$, the Hamiltonian (1) becomes

$$\hat{H}_S = \Delta_a\hat{a}^\dagger\hat{a} + \Delta_b\hat{b}^\dagger\hat{b} + g(\hat{a}\hat{b}^\dagger + \hat{a}^\dagger\hat{b}) + G(\hat{a}^{\dagger 2} + \hat{a}^2) + F^*\hat{b} + F\hat{b}^\dagger, \tag{2}$$

where $\Delta_a = \omega_a - \omega_l$ and $\Delta_b = \omega_b - \omega_l$ denote the detunings of the left and right cavities from the driving field, respectively. Below, we assume $\Delta_a = \Delta_b \equiv \Delta$. Here we note that the phase θ in $G(e^{-i2\theta}\hat{a}^{\dagger 2} + e^{2i\theta}\hat{a}^2)$ of Eq. (1) can be absorbed into the relative phase $\varphi - \theta$ in $fe^{i(\phi-\theta)}\hat{b} + fe^{-i(\phi-\theta)}\hat{b}^\dagger$ found by the transformation $\hat{a} \rightarrow \hat{a}e^{-i\theta}$ and $b \rightarrow \hat{b}e^{-i\theta}$. Therefore, we do not consider the phase θ in the paper. In addition to the unitary evolution governed by the Hamiltonian $\hat{H}_S$ in Eq. (2), there is a loss due to photons leaking out of the right cavity, which is governed by the Markovian master equation

$$\dot{\rho}_S = -i[\hat{H}_S, \rho_S] + \gamma\left(\hat{b}\rho_S\hat{b}^\dagger - \tfrac{1}{2}\hat{b}^\dagger\hat{b}\rho_S - \tfrac{1}{2}\rho_S\hat{b}^\dagger\hat{b}\right), \tag{3}$$

where γ denotes the dissipation for the right cavity. Moreover, the discussion of imposing the dissipation to the left cavity can be found in Sec. VI.

The photon statistical properties of the left cavity can be characterized by the steady second-order correlation function

$$g^{(2)}(0) = \frac{\langle \hat{a}^\dagger \hat{a}^\dagger \hat{a}\hat{a}\rangle}{\langle \hat{a}^\dagger \hat{a}\rangle^2} = \frac{\mathrm{Tr}_S(\hat{a}^\dagger \hat{a}^\dagger \hat{a}\hat{a}\bar{\rho}_S)}{[\mathrm{Tr}_S(\hat{a}^\dagger \hat{a}\bar{\rho}_S)]^2}, \tag{4}$$

where $\bar{\rho}_S$ denotes the steady density matrix satisfying $\dot{\bar{\rho}}_S = 0$ in Eq. (3). The conditions $g^{(2)}(0) < 1$ and $g^{(2)}(0) > 1$ correspond to the photon antibunching and bunching effects, respectively. The limit $g^{(2)}(0) \to 0$ indicates the photon blockade of the left cavity, where only one photon can be excited in the left cavity.

B. Optimal condition for UPB

In order to give the optimal condition for the photon antibunching and understand the origin of UPB with the non-Markovian effect, we consider only the zero-, one-, and two-photon states under the weak driving condition. Assuming that the system is initially prepared in the vacuum state $|0,0\rangle$, the steady state of the system can be written as [27,89]

$$\begin{aligned}|\bar{\psi}\rangle = {}& \bar{E}_{00}|0,0\rangle + \bar{E}_{01}|0,1\rangle + \bar{E}_{10}|1,0\rangle \\ & + \bar{E}_{11}|1,1\rangle + \bar{E}_{02}|0,2\rangle + \bar{E}_{20}|2,0\rangle,\end{aligned} \tag{5}$$

where $\bar{E}_{mn}$ denotes the steady probability amplitude on $|m,n\rangle = |m\rangle_a \otimes |n\rangle_b$ with the left and right cavities respectively having m and n photons.

Under the weak driving condition, we have $|\bar{E}_{00}| \gg |\bar{E}_{10}|, |\bar{E}_{01}| \gg |\bar{E}_{11}|, |\bar{E}_{02}|, |\bar{E}_{20}|$. With Eqs. (4) and (5), the steady second-order correlation function $g^{(2)}(0) \simeq \langle\bar{\psi}|\hat{a}^\dagger\hat{a}^\dagger\hat{a}\hat{a}|\bar{\psi}\rangle/\langle\bar{\psi}|\hat{a}^\dagger\hat{a}|\bar{\psi}\rangle^2 \simeq 2|\bar{E}_{20}|^2/|\bar{E}_{10}|^4 = 0$ by setting $\bar{E}_{20} = 0$ in Eq. (B1) leads to the optimal condition

$$\begin{aligned}\Delta_{\mathrm{opt}} &= \pm\sqrt{\mathcal{Y}},\\ \sin 2\phi_{\mathrm{opt}} &= \frac{G\gamma\left[2(10g^2-\gamma^2)\Delta_{\mathrm{opt}}^2 - 32\Delta_{\mathrm{opt}}^4 + g^2 l_{0.5}\right]}{2f^2g^2\left(\gamma^2+16\Delta_{\mathrm{opt}}^2\right)},\\ \cos 2\phi_{\mathrm{opt}} &= \frac{G\left[(32g^4 - l_1\gamma^2)\Delta_{\mathrm{opt}} - 12 l_1\Delta_{\mathrm{opt}}^3 + 64\Delta_{\mathrm{opt}}^5\right]}{4f^2g^2\left(\gamma^2+16\Delta_{\mathrm{opt}}^2\right)},\end{aligned} \tag{6}$$

with $l_x = \gamma^2 + 8xg^2$ and $\mathcal{Y}$ being determined by the quintic equation

$$\bar{m}\mathcal{Y}^5 + \bar{n}\mathcal{Y}^4 + \bar{o}\mathcal{Y}^3 + \bar{p}\mathcal{Y}^2 + \bar{q}\mathcal{Y} + \bar{r} = 0, \tag{7}$$

where the expressions for these coefficients $\bar{m}$, $\bar{n}$, $\bar{o}$, $\bar{p}$, $\bar{q}$, $\bar{r}$ and derivation of Eq. (6) can be found in Appendix B. We point out that the vanishing population on the two-photon state $|2,0\rangle$ occurs and then the strong photon antibunching can be obtained [i.e., $g^{(2)}(0) \to 0$] if the detuning Δ and phase ϕ simultaneously take their optimal values $\Delta = \Delta_{\mathrm{opt}}$ and $\phi = \phi_{\mathrm{opt}}$ in Eq. (6), otherwise the left cavity is not in the strong photon antibunching regime. The optimal condition (6) for strong photon antibunching photons of the left cavity depends on the controllable parameters of the system such as the frequency detuning Δ, the loss γ, and the phase ϕ with the other parameters g, G, and f fixed.

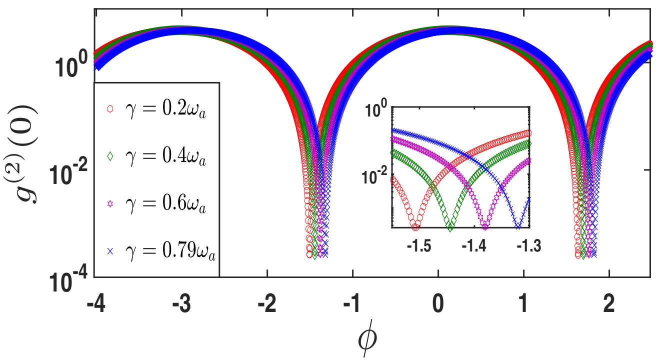

FIG. 2. The influences of the dissipation γ on UPB with the second-order correlation function [$g^{(2)}(0)$ in log scale] as a function of the phase ϕ (in units of rad) by numerically solving master equation (3). Δ takes its negative optimal value, i.e., $\Delta_{\mathrm{opt}} = (-1.597\,82\omega_a,\ -1.591\,49\omega_a,\ -1.580\,92\omega_a,\ -1.566\,97\omega_a)$ respectively corresponding to $\gamma = (0.2\omega_a,\ 0.4\omega_a,\ 0.6\omega_a,\ 0.79\omega_a)$. The other parameters chosen are $g = 0.2\omega_a$, $G = 0.0001\omega_a$, and $f = 0.1\omega_a$.

We use the optimal condition in Eq. (6) and second-order correlation function $g^{(2)}(0)$ by numerically solving master equation (3) as a function of the phase ϕ with different dissipation γ to understand the extreme points in Figs. 2–5. Here we show that the optimal parameters $(\Delta_{\mathrm{opt}}, \phi_{\mathrm{opt}})$ have four real solutions within a period for the optimal phase $(-\pi \leqslant \phi_{\mathrm{opt}} \leqslant \pi)$, e.g., $(\Delta_{\mathrm{opt}}, \phi_{\mathrm{opt}})$=$(-1.597\,82\omega_a, -1.507\,42\ \mathrm{rad})$, $(-1.597\,82\omega_a, 1.634\,16\ \mathrm{rad})$, $(1.597\,82\omega_a, -0.063\,36\ \mathrm{rad})$, and $(1.597\,82\omega_a, 3.078\,22\ \mathrm{rad})$ for the dissipation $\gamma = 0.2\omega_a$ with the other parameters fixed in Figs. 2 and 3. Similar situations exist in other figures. In Figs. 2 and 3, we find that the phase ϕ corresponding to the second-order correlation function arriving at its minimum is shifted with the change of the dissipation γ. To be specific, the position of ϕ moves right with the increase of dissipation γ under $\Delta_{\mathrm{opt}} \leqslant 0$ in Fig. 2, while the position of ϕ deviates left with the increase of dissipation γ under $\Delta_{\mathrm{opt}} \geqslant 0$ in Fig. 3. Moreover, the second-order correlation function $g^{(2)}(0)$ clearly shows that the antibunching effect occurs when the dissipation γ is not

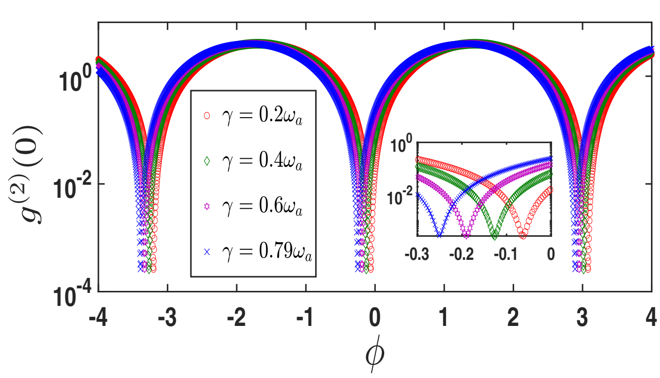

FIG. 3. The figure [$g^{(2)}(0)$ in log scale] shows the case of taking the positive optimal detuning $\Delta_{\mathrm{opt}} = (1.597\,82\omega_a, 1.591\,49\omega_a, 1.580\,92\omega_a, 1.566\,97\omega_a)$ vs $\gamma = (0.2\omega_a, 0.4\omega_a, 0.6\omega_a, 0.79\omega_a)$. The phase ϕ is in units of rad. The other parameters chosen are the same as those in Fig. 2.

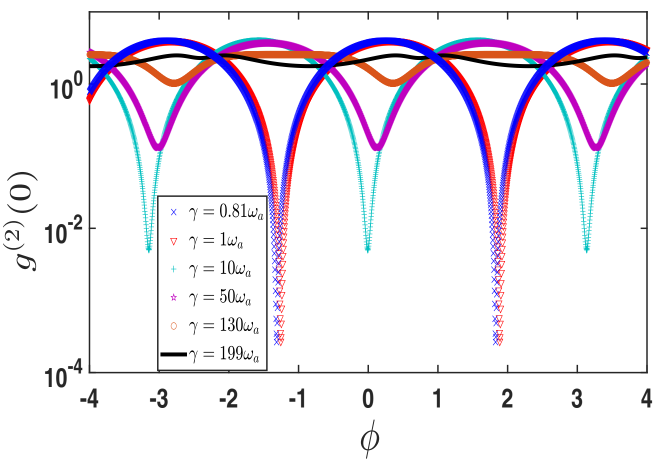

FIG. 4. The influences of the large dissipation $\gamma = (0.81\omega_a, 1\omega_a, 10\omega_a, 50\omega_a, 130\omega_a, 199\omega_a)$ on UPB [$g^{(2)}(0)$ in log scale], where the negative optimal detuning $\Delta_{\text{opt}} = (-1.565\,28\omega_a, -1.547\,12\omega_a, -0.159\,64\omega_a, -0.006\,20\omega_a, -0.000\,72\omega_a, -0.000\,04\omega_a)$. The phase ϕ is in units of rad. The other parameters chosen are the same as those in Fig. 2.

too large, e.g., $\gamma < 0.8\omega_a$ and $g^{(2)}(0)$ arrives at 10^{-4}, where the photon antibunching effect of the system becomes very obvious with small dissipation γ. This indicates that the photon blockade effect in our system can be used to convert the coherent driving pump laser into a single-photon stream.

In Figs. 4 and 5, there is also a phenomenon of the phase ϕ shifted by adjusting the detuning $\Delta_{\text{opt}} \leqslant 0$ or not. However, an important difference compared with Figs. 2 and 3 is that the minimum value of $g^{(2)}(0)$ becomes higher with the increase of dissipation γ, where the minimum value of $g^{(2)}(0)$ arrives at $g^{(2)}(0) \geqslant 1$ when the dissipation γ is large enough. We find that the antibunching effect not only can be obtained, but also the strong bunching effect can be observed in optimal regimes, which leads to controllability of UPB by adjusting the value of the dissipation γ.

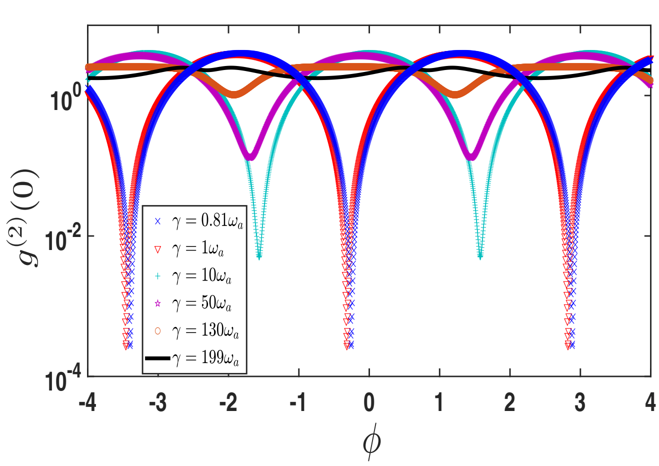

FIG. 5. The figure [$g^{(2)}(0)$ in log scale] shows the case of the positive optimal detuning $\Delta_{\text{opt}} = (1.565\,28\omega_a, 1.547\,12\omega_a, 0.159\,64\omega_a, 0.006\,20\omega_a, 0.000\,72\omega_a, 0.000\,04\omega_a)$ vs $\gamma = (0.81\omega_a, 1\omega_a, 10\omega_a, 50\omega_a, 130\omega_a, 199\omega_a)$. The phase ϕ is in units of rad. The other parameters chosen are the same as Fig. 4.

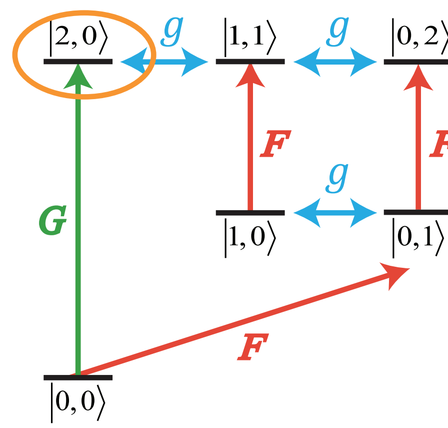

FIG. 6. Energy-level diagram with the zero-, one-, and two-photon states and transition paths leading to the quantum interference responsible for the strong photon antibunching. For the left cavity, the destructive quantum interference processes occur in the following two paths: (i) the direct excitation via two-photon pump in Eq. (8) and (ii) the indirect transitions by single-photon driving field and tunneling coupling in Eqs. (9) and (10).

C. Physical origin of strong photon antibunching

In Fig. 6, we show the energy levels and transition paths, which are produced by two-photon pump and single-photon driving field, respectively. The physical origin of strong photon antibunching is the destructive interference between direct and indirect paths of two-photon excitations, i.e.,

$$|0,0\rangle \xrightarrow{G} |2,0\rangle, \tag{8}$$

$$|0,0\rangle \xrightarrow{F} |0,1\rangle \xrightarrow{F} |0,2\rangle \xrightarrow{g} |1,1\rangle \xrightarrow{g} |2,0\rangle, \tag{9}$$

$$|0,0\rangle \xrightarrow{F} |0,1\rangle \xrightarrow{g} |1,0\rangle \xrightarrow{F} |1,1\rangle \xrightarrow{g} |2,0\rangle, \tag{10}$$

which lead to a closed quantum interference path forming and are responsible for the strong photon antibunching. In this case, the destructive interference occurs when the contributions of states $|0,0\rangle$ and $|1,1\rangle$ to the two-photon state $|2,0\rangle$ exactly cancel each other, i.e., $G\bar{E}_{00} + g\bar{E}_{11} = 0$ (or $\bar{E}_{11} = -G\bar{E}_{00}/g$), together with the fifth equation of Eq. (B1)

$$\sqrt{2}G\bar{E}_{00} + \sqrt{2}g\bar{E}_{11} + 2\Delta\bar{E}_{20} = 0, \tag{11}$$

inducing two-photon probability amplitude $\bar{E}_{20} = 0$. The condition for the coefficients $\bar{E}_{00}$, $\bar{E}_{01}$, $\bar{E}_{10}$, and $\bar{E}_{02}$ in Eq. (B1) to have nontrivial solutions is that the determinant of the coefficient matrix

$$\begin{pmatrix} F & \Delta - i\gamma/2 & g & 0 \\ 0 & g & \Delta & 0 \\ G(i\gamma/2 - 2\Delta)/g & 0 & F & \sqrt{2}g \\ -\sqrt{2}G & \sqrt{2}F & 0 & 2\Delta - i\gamma \end{pmatrix} \tag{12}$$

equals zero, which results in the optimal condition (B2). Moreover, if the system parameters satisfy the optimal condition (6), the destructive interference occurs, which causes the vanishing population on the two-photon state $|2,0\rangle$.

To be specific, with $\gamma = 0.2\omega_a$, $g = 0.2\omega_a$, $G = 0.0001\omega_a$, and $f = 0.1\omega_a$, we obtain the optimal parameters through

Eq. (6) as $(\Delta_{\rm opt}, \phi_{\rm opt})$=$(-1.597\,82\omega_a, -1.507\,42$ rad), $(-1.597\,82\omega_a, 1.634\,16$ rad), $(1.597\,82\omega_a, -0.063\,36$ rad), and $(1.597\,82\omega_a, 3.078\,22$ rad) within $(-\pi \leqslant \phi_{\rm opt} \leqslant \pi)$. With the fixed optimal detuning $\Delta_{\rm opt} = -1.597\,82\omega_a$, we find that the second-order correlation function $g^{(2)}(0)$ gets the minimum values 2.628×10^{-4} and 2.58×10^{-4} at two optimized phases $\phi = -1.507\,42$ and $1.634\,16$ rad in the red circle of Fig. 2, where both sets of parameters $\Delta_{\rm opt} = -1.597\,82\omega_a$ and $\phi = -1.507\,42$ rad as well as $\Delta_{\rm opt} = -1.597\,82\omega_a$ and $\phi = 1.634\,16$ rad meet the optimal condition (6), i.e., $\sin 2\phi = G\gamma[2(10g^2 - \gamma^2)\Delta_{\rm opt}^2 - 32\Delta_{\rm opt}^4 + g^2 l_{0.5}]/[2f^2g^2(\gamma^2 + 16\Delta_{\rm opt}^2)] = -0.126$ and $\cos 2\phi = G[(32g^4 - l_1\gamma^2)\Delta_{\rm opt} - 12l_1\Delta_{\rm opt}^3 + 64\Delta_{\rm opt}^5]/[4f^2g^2(\gamma^2 + 16\Delta_{\rm opt}^2)] = -0.992$, which lead to the destructive interference occurring [as a consequence, $G\bar{E}_{00} + g\bar{E}_{11} = 0$, $\bar{E}_{20} = 0$, and $g^{(2)}(0) = 0$]. For the fixed optimal detuning $\Delta_{\rm opt} = 1.597\,82\omega_a$, two optimal phases $\phi = -0.063\,36$ and $3.078\,22$ rad also satisfying Eq. (6) can be respectively observed at the minimum values of the second-order correlation function in the red circle of Fig. 3.

At the nonoptimized phases in the red circle of Fig. 2 with the fixed optimal detuning $\Delta_{\rm opt} = -1.597\,82\omega_a$, e.g., $\phi = 0$, the second-order correlation function $g^{(2)}(0) = 3.982$ corresponds to the photon bunching effect. This originates from the fact that two paths composed of $|0, 0\rangle$ and $|1, 1\rangle$ do not induce the destructive interference [consequently, $G\bar{E}_{00} + g\bar{E}_{11} \neq 0$, $\bar{E}_{20} \neq 0$, and $g^{(2)}(0) \neq 0$], where the parameters $\Delta_{\rm opt} = -1.597\,82\omega_a$ and $\phi = 0$ violate the optimal condition (6), i.e., $\sin 2\phi = 0$ does not equal $G\gamma[2(10g^2 - \gamma^2)\Delta_{\rm opt}^2 - 32\Delta_{\rm opt}^4 + g^2 l_{0.5}]/[2f^2g^2(\gamma^2 + 16\Delta_{\rm opt}^2)] = -0.126$, and $\cos 2\phi = 1$ does not equal $G[(32g^4 - l_1\gamma^2)\Delta_{\rm opt} - 12l_1\Delta_{\rm opt}^3 + 64\Delta_{\rm opt}^5]/[4f^2g^2(\gamma^2 + 16\Delta_{\rm opt}^2)] = -0.992$.

III. EXACT NON-MARKOVIAN HEISENBERG-LANGEVIN EQUATION FOR THE LEFT CAVITY

Through the equivalence between the Markovian master equation (3) and Heisenberg-Langevin equation (C1) for the environment being initially prepared in the vacuum state (see Appendix C for more details), we can derive the exact non-Markovian Heisenberg-Langevin equation for the left cavity. To be specific, the system operator $\hat{A}(t) = e^{i\hat{H}_T t}\hat{A}(0)e^{-i\hat{H}_T t}$ satisfies the Heisenberg-Langevin equation (C1) with

$$\hat{H}_T = \hat{H}_S + \hat{H}_R + \hat{H}_I, \tag{13}$$

where $\hat{H}_I = i\sum_k V_k(\hat{e}_k^\dagger\hat{b} - \hat{b}^\dagger\hat{e}_k)$ (interaction Hamiltonian between right cavity and Markovian environment with coupling strength $V_k = \sqrt{\gamma/2\pi}$ and decay rate γ), $\hat{H}_R = \sum_k(\omega_k - \omega_l)\hat{e}_k^\dagger\hat{e}_k$ (free Hamiltonian of Markovian environment) with $[\hat{e}_k, \hat{e}_{k'}^\dagger] = \delta_{kk'}$. $\hat{H}_S$ in Eq. (13) is determined by Eq. (2). Equation (C1) gives

$$\frac{d}{dt}\hat{a} = -i\Delta\hat{a} - ig\hat{b} - 2iG\hat{a}^\dagger, \tag{14}$$

$$\frac{d}{dt}\hat{b} = -i\Delta\hat{b} - ig\hat{a} - iF - \frac{\gamma}{2}\hat{b} - \sqrt{\gamma}\hat{e}_{\rm in}(t), \tag{15}$$

where $\hat{e}_{\rm in}(t) = \sum_k e^{-i(\omega_k-\omega_l)t}\hat{e}_k/\sqrt{2\pi}$ meets $[\hat{e}_{\rm in}(t), \hat{e}_{\rm in}^\dagger(t')] = \langle\hat{e}_{\rm in}(t)\hat{e}_{\rm in}^\dagger(t')\rangle = \delta(t - t')$ with the environment initially being prepared in the vacuum state. Solving Eq. (15) for $\hat{b}(t)$ yields $\hat{b}(t) = \hat{b}(0)e^{-(i\Delta+\frac{\gamma}{2})t} - ig\int_0^t \hat{a}(\tau)e^{-(i\Delta+\frac{\gamma}{2})(t-\tau)}d\tau - iF\int_0^t e^{-(i\Delta+\frac{\gamma}{2})(t-\tau)}d\tau - \sqrt{\gamma}\int_0^t \hat{e}_{\rm in}(\tau)e^{-(i\Delta+\frac{\gamma}{2})(t-\tau)}d\tau$. Substituting $\hat{b}(t)$ into Eq. (14), we obtain

$$\frac{d}{dt}\hat{a} = -i\Delta\hat{a} - 2iG\hat{a}^\dagger - \int_0^t f(t-\tau)\hat{a}(\tau)d\tau - iF_{\rm eff}(t) - i\hat{R}(t), \tag{16}$$

where the operator for the non-Markovian composite environment (including right cavity plus its Markovian environment) $\hat{R}(t) = g\hat{b}(0)e^{-(i\Delta+\frac{\gamma}{2})t} - g\sqrt{\gamma}\int_0^t \hat{e}_{\rm in}(\tau)e^{-(i\Delta+\frac{\gamma}{2})(t-\tau)}d\tau$, memory function $f(t) = g^2e^{-(i\Delta+\frac{\gamma}{2})t}$, and effective single-photon driving field $F_{\rm eff}(t) = -igF\int_0^t e^{-(i\Delta+\frac{\gamma}{2})(t-\tau)}d\tau$. Considering the linearity of Eq. (16), the cavity operator $\hat{a}(t)$ can be expressed in terms of the initial operators as

$$\hat{a}(t) = u(t)\hat{a}(0) + v(t)\hat{a}^\dagger(0) + \hat{c}(t), \tag{17}$$

where the time-dependent coefficients are determined by substituting Eq. (17) into Eq. (16):

$$\begin{aligned}\dot{u}(t) &= -i\Delta u(t) - \int_0^t f(t-\tau)u(\tau)d\tau - 2iGv^*(t),\\ \dot{v}(t) &= -i\Delta v(t) - \int_0^t f(t-\tau)v(\tau)d\tau - 2iGu^*(t),\\ \frac{d}{dt}\hat{c}(t) &= -i\Delta\hat{c}(t) - \int_0^t f(t-\tau)\hat{c}(\tau)d\tau - 2iG\hat{c}^\dagger(t)\\ &\quad - iF_{\rm eff}(t) - i\hat{R}(t),\end{aligned} \tag{18}$$

subjected to the initial condition $u(0) = 1$, $v(0) = 0$, and $\hat{c}(0) = 0$. $\hat{c}(t)$ can be analytically derived from the inhomogeneous integrodifferential equation (18):

$$\hat{c}(t) = \hat{\alpha}(t) + \beta(t), \tag{19}$$

where the dissipation and coherent contribution $\hat{\alpha}(t) = i\int_0^t d\tau[v(t-\tau)\hat{R}^\dagger(\tau) - u(t-\tau)\hat{R}(\tau)]$ and $\beta(t) = i\int_0^t d\tau[v(t-\tau)F_{\rm eff}^*(t) - u(t-\tau)F_{\rm eff}(t)]$, respectively. The first term $\hat{\alpha}(t)$ and second term $\beta(t)$ of Eq. (19) denote the influences of the non-Markovian composite environment (right cavity plus its Markovian environment) and effective single-photon driving field on the dynamics for the left cavity, respectively. One is that the driving field forces the left cavity to tend to coherence, while the other is that the non-Markovian composite environment causes the system to dissipate. When the left cavity interacts with the composite environment composed of the right cavity (i.e., as a pseudomode [201–213]) and a Markovian environment, the dynamics of the left cavity behaves as the dissipation or the backflow oscillation of the photon from the composite environment, where the former corresponds to the Markovian approximation, while the latter exhibits non-Markovian effects. The derivation of Eq. (19) can be found in Appendix D.

In Fig. 7, we plot the transition paths of the left cavity with the non-Markovian regime and Markovian limit. Two transitions can form the destructive quantum interference paths when the dissipation γ is small enough in the non-Markovian regime with the second-order correlation function $g^{(2)}(0) \ll 1$

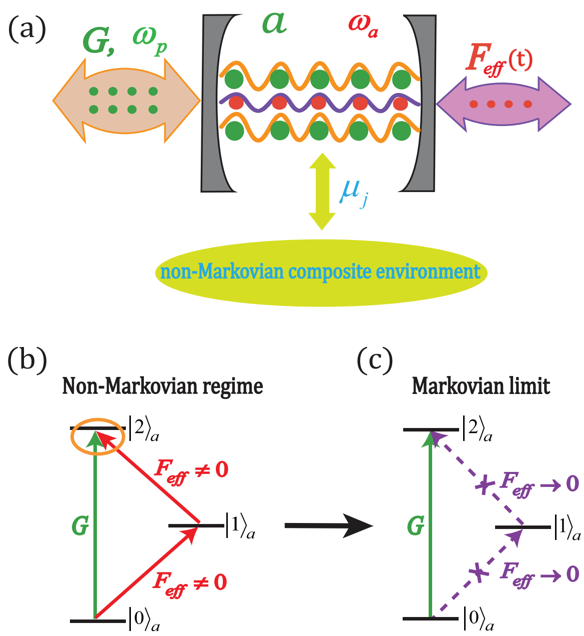

FIG. 7. (a) The two-photon pump and single-photon driving field respectively mediating the dissipationless left cavity and Markovian dissipative right cavity are equivalent to the fact that the two-photon pumped left cavity couples with a driven non-Markovian environment [see Eq. (20) and Appendix E for more details]. In other words, the parts outside the left cavity can be considered as a non-Markovian composite environment [right cavity plus its Markovian environment, see Eq. (13)], which corresponds to the pseudomode theory [201–213]. (b) Energy-level diagram of the left cavity with the zero-, one-, and two-photon states and transition paths leading to the quantum interference responsible for the strong photon antibunching. There are two interference paths occurring in the left cavity from $|0\rangle_a$ to $|2\rangle_a$ in the non-Markovian regime: (i) $|0\rangle_a \xrightarrow{G} |2\rangle_a$ excited by two-photon pump with strength G and (ii) $|0\rangle_a \xrightarrow{F_{\rm eff}} |1\rangle_a \xrightarrow{F_{\rm eff}} |2\rangle_a$ driven by effective single-photon driving field with strength $F_{\rm eff}$. However, there is only one path from $|0\rangle_a$ to $|2\rangle_a$ mediated by two-photon pump when the dissipation tends to infinity under the Markovian limit, where $F_{\rm eff}$ is close to zero.

in Fig. 7(b). In the case, the steady effective single-photon driving field equals $\bar{F}_{\rm eff} = -igF/(i\Delta + \gamma/2)$, which meets the interference condition $G = 10^{-4}\omega_a \sim |\bar{F}|^2_{\rm eff} = 1.5 \times 10^{-4}\omega_a^2$ at $\Delta_{\rm opt} = -1.597\,82\omega_a$ and $\gamma = 0.2\omega_a$ for the red circle in Fig. 2. This means photons of the dissipative right cavity could flow back to the left cavity via the coupling strength g, which causes UPB in the non-Markovian regime together with the direct excitation by two-photon pump. With the increase of dissipation γ, especially, when the dissipation γ goes to infinity for the bad cavity limit [214–220] under the Markovian limit, the effective single-photon driving field $F_{\rm eff}$ is close to zero in Fig. 7(c). It indicates that only one transition exists under the Markovian limit and the closed quantum interference path is broken (e.g., $G = 10^{-4}\omega_a \gg |\bar{F}|^2_{\rm eff} = 4 \times 10^{-8}\omega_a^2$ for $\Delta_{\rm opt} = -0.000\,04\omega_a$ and $\gamma = 199\omega_a$ for the black line in Fig. 4), which leads to photon bunching occurring.

IV. EXACT NON-MARKOVIAN MASTER EQUATION FOR THE LEFT CAVITY

In Appendix E, we have proved that the total Hamiltonian (13) is equivalent to the two-photon pumped left cavity interacting with a driven non-Markovian composite environment (consisting of the right cavity plus its Markovian environment), whose Hamiltonian reads

$$\hat{H}_T = \Delta\hat{a}^\dagger\hat{a} + G(\hat{a}^{\dagger 2} + \hat{a}^2) + \sum_j \chi_j\hat{B}_j^\dagger\hat{B}_j + \sum_j \mu_j^*\hat{a}^\dagger\hat{B}_j + \mu_j\hat{B}_j^\dagger\hat{a} + \sum_j \nu_j^*\hat{B}_j + \sum_j \nu_j\hat{B}_j^\dagger, \quad (20)$$

where the dressed annihilation operator $\hat{B}_j$ satisfies the Bosonic orthogonal-normalization relation. The coupling coefficient and driving strength are $\mu_j = g\alpha_j$ and $\nu_j = F\alpha_j$, respectively. α_j and χ_j are determined by Eq. (E4). The initial state (C2) and total Hamiltonian (20) remain linear and Gaussian and allow exact integration [121,128,154,157,221–231], which makes the reduced density matrix $\rho = {\rm Tr}_b\rho_S$ also a Gaussian. With the conservation of trace (${\rm Tr}\dot{\rho} = 0$) and Hermiticity ($\rho = \rho^\dagger$), we obtain the exact reduced non-Markovian master equation for the left cavity:

$$\begin{aligned}\dot{\rho} = &-i[\hat{\mathcal{H}}(t), \rho] \\ &+ \kappa_1(t)\big(\hat{a}\rho\hat{a}^\dagger - \tfrac{1}{2}\hat{a}^\dagger\hat{a}\rho - \tfrac{1}{2}\rho\hat{a}^\dagger\hat{a}\big) \\ &+ \kappa_2(t)\big(\tfrac{1}{2}\hat{a}\rho\hat{a}^\dagger + \tfrac{1}{2}\hat{a}^\dagger\rho\hat{a} - \tfrac{1}{2}\hat{a}^\dagger\hat{a}\rho - \tfrac{1}{2}\rho\hat{a}\hat{a}^\dagger\big) \\ &+ \big[\kappa_3^*(t)\big(\hat{a}\rho\hat{a} - \tfrac{1}{2}\hat{a}\hat{a}\rho - \tfrac{1}{2}\rho\hat{a}\hat{a}\big) + {\rm H.c.}\big], \end{aligned} \quad (21)$$

with the time-dependent effective Hamiltonian

$$\hat{\mathcal{H}}(t) = X(t)\hat{a}^\dagger\hat{a} + [Y(t)\hat{a}^{\dagger 2} + Z(t)\hat{a}^\dagger + {\rm H.c.}], \quad (22)$$

where the time-dependent coefficients in Eq. (21) can be found in Eq. (F3) in Appendix F. Now we discuss the physical meaning of the time-dependent coefficients in the exact non-Markovian master equation (21) as follows.

(i) The first term in Eq. (22) accounts for the free dynamics of the left cavity, where $X(t) = \Delta + \delta\omega(t)$ with $\delta\omega(t) = {\rm Im}[u^*(t)\int_0^t f(t-\tau)u(\tau)d\tau - v^*(t)\int_0^t f(t-\tau)v(\tau)d\tau]/\vartheta(t)$ obtained by Eqs. (18) and (F3) is modified by the frequency shift $\delta\omega(t)$ owing to the left cavity coupling with the composite environment.

(ii) The second term in Eq. (22) denotes the two-photon process, which originates from the two-photon pump (conversion rate G) to the left cavity in Eq. (2).

(iii) The third term in Eq. (22) is a coherent term, which denotes the effective driving to the left cavity, where the effective driving strength $Z(t)$ is affected by the interaction between the left cavity and composite environment.

(iv) $\kappa_1(t)$ in Eq. (21) is a time-dependent damping rate, which denotes the dissipation in the left cavity induced by the composite environment.

(v) $\kappa_2(t)$ in Eq. (21) is the fluctuation (noise) coefficient due to the backreaction between the left cavity and composite environment.

(vi) $\kappa_3(t)$ in Eq. (21) denotes the incoherent two-photon pump rate, which is induced by the interaction between the

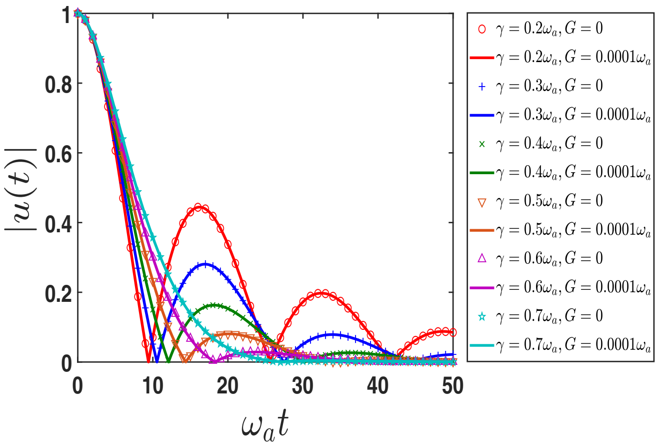

FIG. 8. $|u(t)|$ in Eq. (18) as a function of the time t with different dissipation γ from $0.2\omega_a$ to $0.7\omega_a$, which lies in the non-Markovian regime. The solid lines and circles correspond to $G = 0.0001\omega_a$ and 0, respectively. The other parameters chosen are the same as those in Fig. 2.

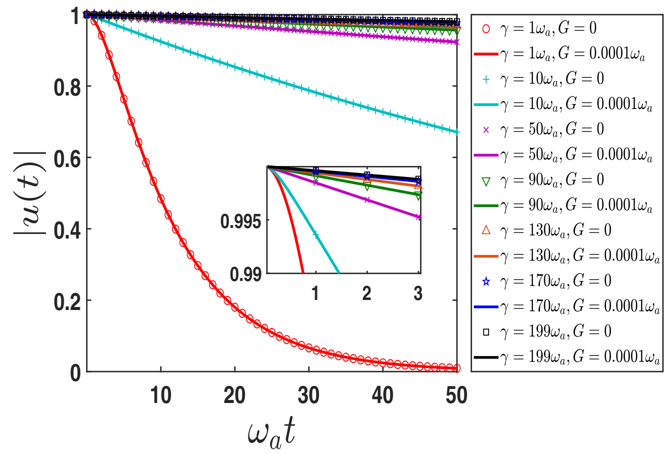

FIG. 10. The figure corresponds to the Markovian regime, where the optimal detuning Δ_{opt} takes negative values. The other parameters chosen are the same as those in Fig. 4.

two-photon pump (conversion rate G) in Eq. (2) and the left cavity.

In order to explain interesting phenomena in the non-Markovian regime in Figs. 2 and 3 compared with those in the Markovian regime in Figs. 4 and 5, we plot $|u(t)|$ in Eq. (18) as a function of the time t with the different dissipation γ in Figs. 8–10, which are discussed as follows.

(i) In Fig. 8, we find that $|u(t)|$ changes from oscillating to damping when the dissipation exceeds a threshold with the fixed two-photon pump $G = 0.0001\omega_a$ (marked by solid lines), which is consistent with that at $G = 0$ (marked by circles). This means that the weak two-photon pump has almost no influence on the properties of non-Markovianity for the left cavity. From Eq. (18) with the case for $G = 0$, we have

$$
\begin{aligned}
u(t) &= e^{-0.25t(\gamma+4i\Delta)}\left[\cosh(0.25t\sqrt{\gamma^2-16g^2}) + \frac{\gamma\sinh(0.25t\sqrt{\gamma^2-16g^2})}{\sqrt{\gamma^2-16g^2}}\right], \quad \gamma > 4g,\\
u(t) &= e^{-0.25t(\gamma+4i\Delta)}\left[\cos(0.25t\sqrt{16g^2-\gamma^2}) + \frac{\gamma\sin(0.25t\sqrt{16g^2-\gamma^2})}{\sqrt{16g^2-\gamma^2}}\right], \quad \gamma < 4g,\\
u(t) &= e^{-t(g+i\Delta)}(1+gt), \quad \gamma = 4g,
\end{aligned}
\tag{23}
$$

which indicate the existence of a threshold $\gamma_{\text{cr}} = 4g$. With $g = 0.2\omega_a$, the threshold is calculated as $\gamma_{\text{cr}} = 0.8\omega_a$, which can also be numerically confirmed by Figs. 8–10. In the non-Markovian regime $\gamma < 0.8\omega_a$, the left cavity is affected by the non-Markovian behavior [$|u(t)|$ exhibits the oscillation] in Figs. 8 and 9(a)–9(c), where there are photons coming from the right cavity backflow to the left cavity and UPB occurs in the non-Markovian regime in Figs. 2 and 3. This phenomenon can also be explained from the perspective of non-Markovian composite environmental memory time. The Lorentzian spectral density $J(\omega)$ corresponding to the memory function $f(t) = g^2 e^{-(i\Delta+\frac{\gamma}{2})t} \equiv \int J(\omega)e^{-i\omega t}d\omega$ in Eq. (16) reads

$$
J(\omega) = \frac{\Gamma}{2\pi}\frac{\lambda^2}{(\omega-\Delta)^2+\lambda^2}, \tag{24}
$$

where $\lambda = \gamma/2$ and $\Gamma = 4g^2/\gamma$. The parameter λ defines the spectral width of the non-Markovian composite environment [136–143,185], which is connected to the non-Markovian composite environment memory time $T_E = \lambda^{-1}$, while the time scale T_S on the state of the system changing is given by $T_S = \Gamma^{-1}$.

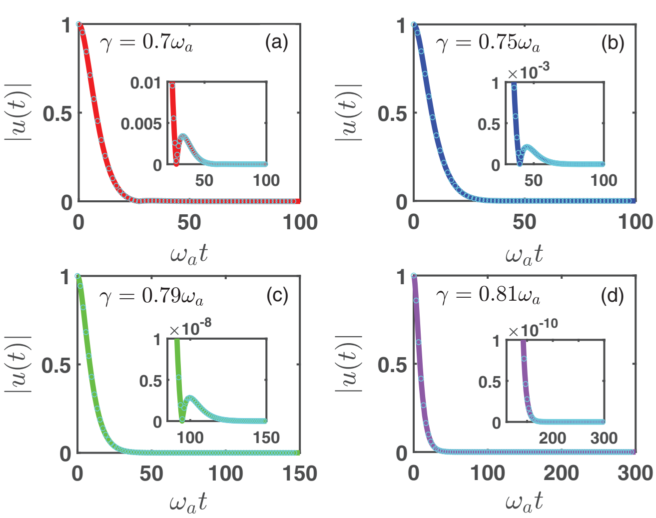

FIG. 9. $|u(t)|$ as a function of the time t with different dissipation γ taking $0.7\omega_a$ $0.75\omega_a$, $0.79\omega_a$, and $0.81\omega_a$ near the threshold $\gamma = 0.8\omega_a$. The circles and solid lines correspond to Eq. (23) for $G = 0$ and Eq. (18) for $G = 0.0001\omega_a$, respectively. With Figs. 8 and 9, we find that $|u(t)|$ exhibits the backflow oscillation of the photon from the non-Markovian composite environment for $\gamma < 0.8\omega_a$, while it displays decay in the Markovian regime when $\gamma > 0.8\omega_a$. The other parameters chosen are the same as those in Fig. 2.

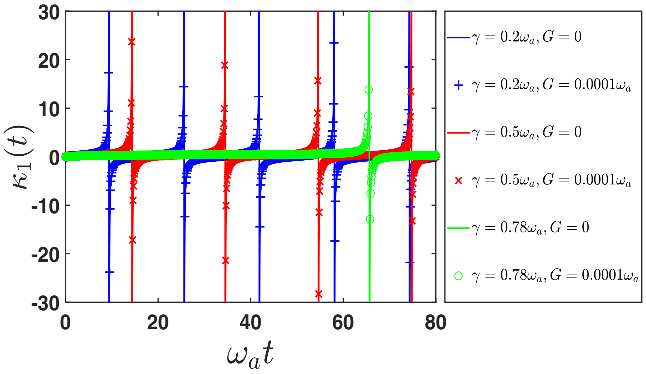

FIG. 11. The dissipation rate $\kappa_1(t)$ in Eq. (21) of the left cavity as a function of the time t with different dissipation γ taking $0.2\omega_a$, $0.5\omega_a$, and $0.78\omega_a$, which correspond to the non-Markovian regime. The other parameters chosen are the same as those in Fig. 2.

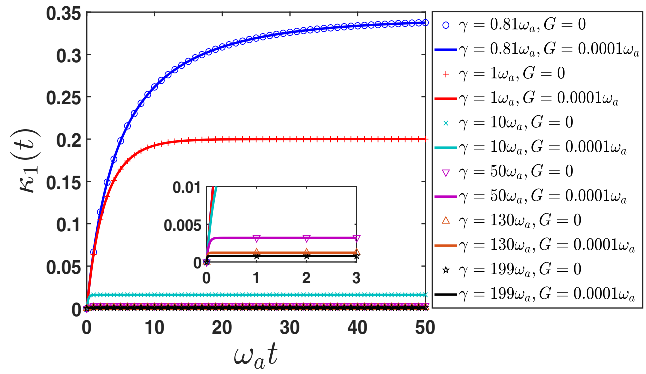

FIG. 12. The figure shows the dissipation rate $\kappa_1(t)$ in Eq. (21) in the Markovian regime, where the optimal detuning Δ_{opt} takes negative values. The other parameters chosen are the same as those in Fig. 4.

When the memory time T_E of the non-Markovian composite environment is comparable to characteristic time T_S of the system (i.e., $T_E \sim T_S$) in the non-Markovian regime, the memory effect of the non-Markovian composite environment should be taken into account and the dynamics of the left cavity exhibits the backflow oscillation of the photon in Figs. 8 and 9(a)–9(c). In this case, the second-order correlation function $g^{(2)}(0)$ clearly shows that UPB occurs and arrives at 10^{-4} in Figs. 2 and 3 with the dissipation $\gamma < 0.8\omega_a$.

(ii) With the increase of dissipation to $\gamma > 0.8\omega_a$ (beyond the threshold $\gamma_{\text{cr}} = 0.8\omega_a$) in the Markovian regime, the oscillation disappears and damping occurs in Figs. 9(d) and 10, where UPB becomes weak as shown in Figs. 4 and 5. Especially, UPB disappears and photon bunching $[g^{(2)}(0) > 1]$ appears when the dissipation takes a sufficiently large value $\gamma = 199\omega_a$ shown in black solid line in Figs. 4 and 5. This is because under the Markovian limit $T_E \ll T_S$ (leading to $\gamma \gg g$, i.e., the memory time T_E of the non-Markovian composite environment is sufficiently shorter than characteristic time T_S of the system), we show $f(t) \to 0$, $F_{\text{eff}}(t) \to 0$, $\hat{R}(t) \to 0$ in Eq. (16), and $|u(t)| \to 1$ in Eq. (18) when the dissipation approaches infinity ($\gamma \to \infty$) in the bad cavity limit [214–220]. In this case, there is no effective dissipation in the left cavity, but only a two-photon pump exists, i.e., $\dot{\rho}_S = -i[\Delta\hat{a}^\dagger\hat{a} + G(\hat{a}^{\dagger 2} + \hat{a}^2), \rho_S]$.

(iii) From the above discussions in (i) and (ii), we find that the dissipation γ can characterize the properties of the non-Markovian composite environment [136–143,185]. On both sides of the threshold $\gamma_{\text{cr}} = 0.8\omega_a$, it can be determined whether the left cavity is non-Markovian or Markovian, which is the reason for the division between antibunching and bunching. In other words, UPB occurs in the non-Markovian regime ($\gamma < 0.8\omega_a$), while it becomes weak for the dissipation $\gamma > 0.8\omega_a$ and then disappears if $\gamma \gg 0.8\omega_a$ (e.g., $\gamma = 199\omega_a$) in the Markovian regime.

(iv) Our purpose in deriving non-Markovian master equation (21) is to demonstrate that a coupled-cavities system with the dissipation γ leads to an exact non-Markovian master equation for the left cavity, which can explain the photon blockade phenomena in Figs. 2–5 with non-Markovian effects through Figs. 11–13. To be specific, the dissipation rate $\kappa_1(t)$ in the exact non-Markovian master equation (21) is a periodic function of time in Fig. 11 and takes negative values sometimes. In particular, $\kappa_1(t)$ has discrete singular points where the left cavity gains photons from the non-Markovian composite environment, which is a typical feature of non-Markovianity [137,160,161,177,178]. With the increase of the dissipation γ (greater than $0.8\omega_a$) in Fig. 12, $\kappa_1(t)$ varies from oscillation to a finite steady value. When the dissipation γ goes to infinity, the dissipation rate $\kappa_1(t)$ and single-photon driving field $F_{\text{eff}}(t)$ tend to zero, which corresponds to the Markovian limit and means no photons flow back to the left cavity, where the photon bunching effect happens. Moreover, we find that the two-photon term $|Y(t)|$ is close to the square of coherent driving term $|Z(t)|$ in Fig. 13(a), which leads to the forming of the destructive quantum interference paths in Fig. 2 [UPB appears in the minimum value of $g^{(2)}(0)$ for the red circle], while $|Y(t)| = 10^{-4}\omega_a \gg |Z(t)|^2 = 10^{-9}\omega_a$ in Fig. 4 breaks the quantum interference paths (photon bunching occurs) in Fig. 13(b).

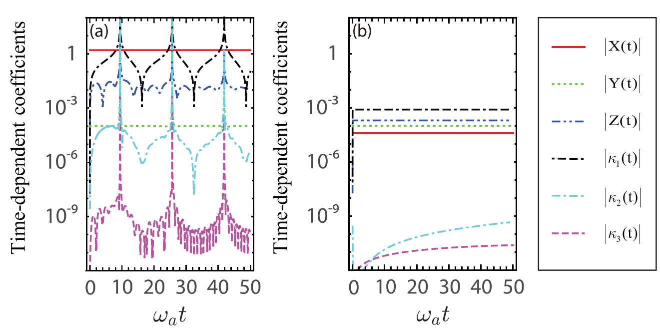

FIG. 13. In order to further understand the origin of UPB for the left cavity with the non-Markovian effect, we in this figure plot the time-dependent coefficients in the exact non-Markovian master equation (21): effective transition frequency $|X(t)|$, two-photon term $|Y(t)|$, coherent driving term $|Z(t)|$, decay rate $|\kappa_1(t)|$, fluctuation (noise) coefficient $|\kappa_2(t)|$, and squeezing rate $|\kappa_3(t)|$ as a function of the time t. Figure 13(a) takes $\Delta_{\text{opt}} = -1.597\,82\omega_a$, $\phi_{\text{opt}} = -1.507\,42$ rad, and $\gamma = 0.2\omega_a$ in Fig. 2, while $\Delta_{\text{opt}} = -0.000\,04\omega_a$, $\phi_{\text{opt}} = -2.406\,19$ rad, and $\gamma = 199\omega_a$ in Fig. 4 correspond to Fig. 13(b). The other parameters chosen are $g = 0.2\omega_a$, $G = 0.0001\omega_a$, and $f = 0.1\omega_a$.

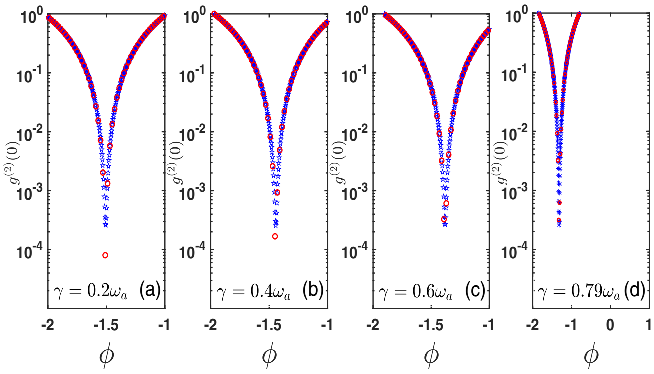

FIG. 14. The second-order correlation function [$g^{(2)}(0)$ in log scale] of the left cavity as a function of the phase ϕ (in units of rad) with the different dissipations $\gamma = 0.2\omega_a$, $0.4\omega_a$, $0.6\omega_a$, and $0.79\omega_a$ for (a)–(d) in the non-Markovian regime. The red circles indicate the approximate analytical result (26), while the blue stars correspond to the numerical simulation by solving master equation (3). The other parameters chosen are the same as those in Fig. 2.

V. ANALYTICAL EXPRESSIONS FOR THE SECOND-ORDER CORRELATION FUNCTION

In this section, we derive an approximate analytical expression for the second-order correlation function and compare it with the numerical simulation by solving master equation (3). To approximately obtain the analytical solution of the second-order correlation function, we need to estimate Eq. (3). Under the weak driving condition, we have $|\bar{E}_{00}| \gg |\bar{E}_{10}|$, $|\bar{E}_{01}| \gg |\bar{E}_{11}|$, $|\bar{E}_{02}|$, $|\bar{E}_{20}|$ and assume that the vacuum state is approximately occupied with $\bar{E}_{00} = 1$ in Eq. (B1). By solving Eq. (B1), we obtain $(\Delta - i\gamma/2)\bar{E}_{01} + g\bar{E}_{10} = -F$, $g\bar{E}_{01} + \Delta\bar{E}_{10} = 0$, $F\bar{E}_{10} + (2\Delta - i\gamma/2)\bar{E}_{11} + \sqrt{2}g\bar{E}_{02} + \sqrt{2}g\bar{E}_{20} = 0$, $F\bar{E}_{01} + g\bar{E}_{11} + \sqrt{2}(\Delta - i\gamma/2)\bar{E}_{02} = 0$, and $g\bar{E}_{11} + \sqrt{2}\Delta\bar{E}_{20} = -G$, which lead to

$$\bar{E}_{10} = \frac{gF}{(\Delta - i\gamma/2)\Delta - g^2},$$
$$\bar{E}_{20} = -\frac{G[(\Delta - i\gamma/2)\Delta - g^2](\Delta - i\gamma/2) - g^2F^2}{\sqrt{2}[(\Delta - i\gamma/2)\Delta - g^2]^2}. \tag{25}$$

With Eq. (25), we can obtain the approximate analytical expression of the second-order correlation function:

$$g^{(2)}(0) \simeq \frac{G^2|[(\Delta - i\gamma/2)\Delta - g^2](\Delta - i\gamma/2) - g^2F^2|^2}{g^4F^4}. \tag{26}$$

In order to compare the approximate analytical solution with the numerical solution of the second-order correlation function, we plot $g^{(2)}(0)$ as a function of the phase ϕ in Fig. 14. The red circles indicate the approximate analytical result (26), while the blue stars correspond to the numerical simulation by solving master equation (3). We find that the approximate analytical results of the second-order correlation function show good agreement with those obtained by the numerical simulation.

Our analytical method is developed to find the optimal parameters $(\Delta_{\rm opt}, \phi_{\rm opt})$ that minimize the second-order correlation function where a truncation of the Hilbert space to two photons is used. Therefore the analytical solution (26) of the second-order correlation function is inaccurate when the photon number is large. However, as shown in Fig. 14, the optimal values are the same as those from the numerical solution by solving master equation (3), which demonstrates the feasibility of our analytical method.

From Fig. 14, we observe that the second-order correlation function $g^{(2)}(0)$ has slight differences between the analytical solution and numerical simulation. The reason leading to this difference is that the Hilbert space is truncated into the finite dimension in the analytical derivation. On the other hand, when we substitute the optimal condition given by Eq. (6) into the analytical solution of $g^{(2)}(0)$ in Eq. (26), we find $g^{(2)}(0) \to 0$ due to $\bar{E}_{20} \to 0$ as predicted. However, in the numerical calculation for $g^{(2)}(0)$, the multiphoton state $|m, n\rangle$ $(m + n \geqslant 3)$ is actually occupied with the very small probability in the weak driving limit, which has been ignored in the analytical analysis. Overall, we do not take the multiphoton state $|m, n\rangle$ $(m + n \geqslant 3)$ into account in Eq. (5). This is the essential reason leading to the very small difference between the analytical result and numerical simulation for the second-order correlation function.

VI. DISCUSSION ON THE EXISTENCE OF DISSIPATIONS IN BOTH CAVITIES

Considering the dissipation γ_1 in the left cavity, we give the Markovian master equation for coupled cavities and corresponding non-Markovian Heisenberg-Langevin equation for the left cavity:

$$\dot{\rho}_S = -i[\hat{H}_S, \rho_S] + \gamma_1\left(\hat{a}\rho_S\hat{a}^\dagger - \frac{1}{2}\hat{a}^\dagger\hat{a}\rho_S - \frac{1}{2}\rho_S\hat{a}^\dagger\hat{a}\right) + \gamma\left(\hat{b}\rho_S\hat{b}^\dagger - \frac{1}{2}\hat{b}^\dagger\hat{b}\rho_S - \frac{1}{2}\rho_S\hat{b}^\dagger\hat{b}\right),$$
$$\frac{d}{dt}\hat{a} = -i(\Delta - i\gamma_1/2)\hat{a} - 2iG\hat{a}^\dagger - \int_0^t f(t-\tau)\hat{a}(\tau)d\tau - iF_{\rm eff}(t) - i\hat{R}(t) - \sqrt{\gamma_1}\hat{h}_{\rm in}(t), \tag{27}$$

where $f(t)$, $F_{\rm eff}(t)$, and $\hat{R}(t)$ are the same as those in Eq. (16), and $\hat{h}_{\rm in}(t) = \sum_{k_1} e^{-i(\Omega_{k_1} - \omega_l)t}\hat{h}_{k_1}/\sqrt{2\pi}$ with Ω_{k_1} and $\hat{h}_{k_1}$ respectively denoting the eigenfrequency and annihilation operator of the Markovian environment corresponding to the left cavity. Through the effective non-Hermitian Hamiltonian $\hat{H}_{\rm eff} = \hat{H}_S - i\gamma_1\hat{a}^\dagger\hat{a}/2 - i\gamma\hat{b}^\dagger\hat{b}/2$, we can obtain the optimal condition for UPB occurring,

$$0 = [g^2G - G(\Delta - i\gamma_1/2)(\Delta - i\gamma/2)][(\Delta - i\gamma_1/2) + (\Delta - i\gamma/2)](\Delta - i\gamma/2) + g^2F^2(\Delta - i\gamma/2) - g^4G + g^2F^2(\Delta - i\gamma_1/2) + g^2G(\Delta - i\gamma_1/2)(\Delta - i\gamma/2), \tag{28}$$

under the weak driving condition. Through numerical simulation similar to Secs. II– IV, we find that the dissipation γ_1 in the left cavity has an influence on the optimal values $(\Delta_{\rm opt}, \phi_{\rm opt})$ in Eq. (28) and second-order correlation function $g^{(2)}(0) = {\rm Tr}_S(\hat{a}^\dagger\hat{a}^\dagger\hat{a}\hat{a}\bar{\rho}_S)/[{\rm Tr}_S(\hat{a}^\dagger\hat{a}\bar{\rho}_S)]^2$ [$\bar{\rho}_S$ denotes the

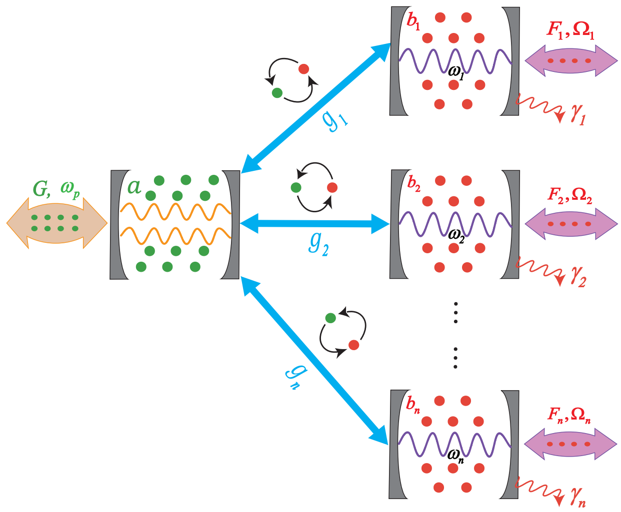

FIG. 15. UPB with the non-Markovian effect for the quantum network can be realized in the dissipationless left cavity (eigenfrequency ω_a) mediated by two-photon pump with amplitude G and frequency ω_p, where the left cavity couples to several dissipative right cavities (eigenfrequency ω_n and dissipation γ_n) with the coupling strength g_n. The right cavity b_n is driven by single-photon driving field with frequency Ω_n and amplitude F_n.

steady density matrix satisfying $\dot{\bar{\rho}}_S = 0$ in Eq. (27)], but it does not change our main conclusions (UPB with the non-Markovian effect) due to the effective single-photon driving field of Eq. (27) remaining finite. We will not discuss it in detail here (readers who are interested in this question can try it out).

VII. DISCUSSION FOR A TWO-PHOTON PUMPED LEFT CAVITY COUPLING WITH NONINTERACTING SINGLE-PHOTON DRIVEN RIGHT CAVITIES

In this section, we generalize the above results to a general quantum network involving several right cavities driven by single-photon driving fields with frequency Ω_n and amplitude F_n in Fig. 15, whose master equation and corresponding total Hamiltonian are given by

$$\dot{\rho}_S = -i[\hat{H}_S, \rho_S] + \sum_n \gamma_n\left(\hat{b}_n\rho_S\hat{b}_n^\dagger - \frac{1}{2}\hat{b}_n^\dagger\hat{b}_n\rho_S - \frac{1}{2}\rho_S\hat{b}_n^\dagger\hat{b}_n\right), \tag{29}$$

and $\hat{H}_T = \hat{H}_S + \hat{H}_R + \hat{H}_I$ with

$$\begin{aligned}\hat{H}_S &= \Delta\hat{a}^\dagger\hat{a} + \sum_n \Delta_n\hat{b}_n^\dagger\hat{b}_n + \sum_n g_n(\hat{a}\hat{b}_n^\dagger + \hat{a}^\dagger\hat{b}_n)\\ &\quad + G(\hat{a}^{\dagger 2} + \hat{a}^2) + \sum_n F_n^*\hat{b}_n + \sum_n F_n\hat{b}_n^\dagger,\\ \hat{H}_R &= \sum_{n,k}(\omega_{n,k} - \Omega)\hat{e}_{n,k}^\dagger\hat{e}_{n,k},\\ \hat{H}_I &= i\sum_{n,k} V_{n,k}(\hat{e}_{n,k}^\dagger\hat{b}_n - \hat{b}_n^\dagger\hat{e}_{n,k}),\end{aligned} \tag{30}$$

where $\Delta = \omega_a - \Omega$, $\Delta_n = \omega_n - \Omega$, and $\hat{e}_{n,\text{in}}(t) = \sum_k e^{-i(\omega_{n,k}-\Omega)t}\hat{e}_{n,k}/\sqrt{2\pi}$. In Eq. (30), we have assumed driving frequency $\Omega_n = \Omega$ and pump frequency $\omega_p = 2\Omega$. g_n denotes coupling strength between the left cavity with frequency ω_a and right cavity b_n with frequency ω_n. $V_{n,k} = \sqrt{\gamma_n/2\pi}$ is the coupling strength between cavity b_n and Markovian environments with Bosonic annihilation operators $\hat{e}_{n,k}$ and frequencies $\omega_{n,k}$. In this case, Eq. (16) becomes

$$\begin{aligned}\frac{d}{dt}\hat{a} = &-i\Delta\hat{a} - 2iG\hat{a}^\dagger - \int_0^t f(t-\tau)\hat{a}(\tau)d\tau\\ &- i\sum_n F_{n,\text{eff}}(t) - i\sum_n \hat{R}_n(t),\end{aligned} \tag{31}$$

where $f(t) = \sum_n g_n^2 e^{-(i\Delta_n + \frac{\gamma_n}{2})t}$, $F_{n,\text{eff}}(t) = -ig_nF_n\int_0^t e^{-(i\Delta_n+\frac{\gamma_n}{2})(t-\tau)}d\tau$, and $\hat{R}_n(t) = g_n\hat{b}_n(0)e^{-(i\Delta_n+\frac{\gamma_n}{2})t} - g_n\sqrt{\gamma_n}\int_0^t \hat{e}_{n,in}(\tau)e^{-(i\Delta_n+\frac{\gamma_n}{2})(t-\tau)}d\tau$. With the linearity of Eq. (31) and defining $\hat{a}(0) \equiv \hat{a}$, $\hat{a}^\dagger(0) \equiv \hat{a}^\dagger$, $\hat{b}_n(0) \equiv \hat{b}_n$, $\hat{b}_n^\dagger(0) \equiv \hat{b}_n^\dagger$, $\hat{e}_{n,k}(0) \equiv \hat{e}_{n,k}$, $\hat{e}_{n,k}^\dagger(0) \equiv \hat{e}_{n,k}^\dagger$, we have

$$\hat{a}(t) = u_1(t)\hat{a}(0) + v_1(t)\hat{a}^\dagger(0) + \hat{c}_1(t), \tag{32}$$

with

$$\begin{aligned}\hat{c}_1(t) = &\sum_n \mu_n(t)\hat{b}_n(0) + \sum_n \nu_n(t)\hat{b}_n^\dagger(0)\\ &+ \sum_{n,k}\alpha_{nk}(t)\hat{e}_{n,k}(0) + \sum_{n,k}\beta_{nk}(t)\hat{e}_{n,k}^\dagger(0) + \eta(t).\end{aligned} \tag{33}$$

The time-dependent functions $u_1(t)$, $v_1(t)$, $\mu_n(t)$, $\nu_n(t)$, $\alpha_{nk}(t)$, $\beta_{nk}(t)$, and $\eta(t)$ in Eq. (33) can be determined by substituting Eq. (32) into Eq. (31):

$$\begin{aligned}\dot{u}_1(t) &= -i\Delta u_1(t) - \int_0^t f(t-\tau)u_1(\tau)d\tau - 2iGv_1{}^*(t),\\ \dot{v}_1(t) &= -i\Delta v_1(t) - \int_0^t f(t-\tau)v_1(\tau)d\tau - 2iGu_1{}^*(t),\\ \frac{d}{dt}\hat{c}_1(t) &= -i\Delta\hat{c}_1(t) - \int_0^t f(t-\tau)\hat{c}_1(\tau)d\tau - 2iG\hat{c}_1^\dagger(t)\\ &\quad - i\sum_n F_{n,\text{eff}}(t) - i\sum_n \hat{R}_n(t).\end{aligned} \tag{34}$$

With the above results, we show that the initial condition and initial state are two different concepts discussed below.

(i) $u_1(0)$ represents an initial condition, whose value is determined by the Heisenberg operator $\hat{a}(t)$ in Eq. (32) at time $t = 0$. To be specific, with $\hat{a}(0) = u_1(0)\hat{a}(0) + v_1(0)\hat{a}^\dagger(0) + \hat{c}_1(0)$ by taking $t = 0$ to $\hat{a}(t) = u_1(t)\hat{a}(0) + v_1(t)\hat{a}^\dagger(0) + \hat{c}_1(t)$, we obtain

$$\begin{aligned}&u_1(0) = 1, \quad v_1(0) = 0, \quad \mu_n(0) = 0,\\ &\nu_n(0) = 0, \quad \alpha_{n,k}(0) = 0, \quad \beta_{n,k}(0) = 0, \quad \eta(0) = 0,\end{aligned} \tag{35}$$

which remain unchanged and are independent of the parameters in Eq. (30). This is a mathematical fact, and therefore $u_1(0) = 1$ is what we must use. However, if $u_1(0) \neq 1$, Eq. (32) will be violated.

(ii) $\rho_S(0)$ denotes the initial state of the master equation (29), which is changeable and can be re-prepared at

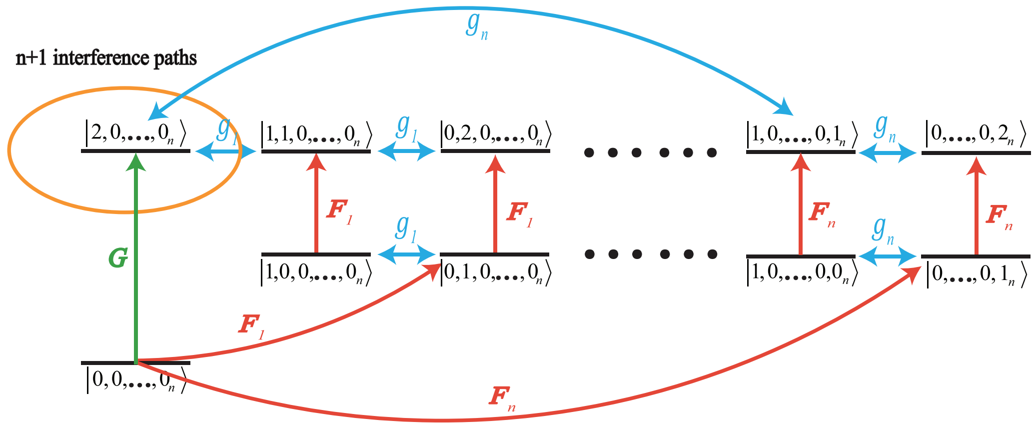

FIG. 16. Energy-level diagram of the quantum network with the zero-, one-, and two-photon states and transition paths leading to the quantum interference responsible for the strong photon antibunching. For the left cavity, the quantum interference processes occur in $n+1$ paths as the figure shows.

the initial time $t=0$. When we reset the cavities, the initial number of photons in the cavities is tunable, which can be realized in experiment [159–161]. In this case, the different initial states $\rho_S(0)$ [being not related to $u_1(t)$] can affect the time-dependent evolution of the system density matrix $\rho_S(t)$ controlled by the master equation (29). But this cannot change the steady state $\bar{\rho}_S$ of the master equation (29) since $\dot{\bar{\rho}}_S=0$ is independent of the initial state. Therefore, the different initial states $\rho_S(0)$ do not affect the steady second-order correlation function $g^{(2)}(0)=\mathrm{Tr}_S(\hat{a}^\dagger\hat{a}^\dagger\hat{a}\hat{a}\bar{\rho}_S)/[\mathrm{Tr}_S(\hat{a}^\dagger\hat{a}\bar{\rho}_S)]^2$.

Moreover, we make the Laplace transformation to Eq. (34) and get

$$\hat{c}_1(t)=\hat{\mathcal{A}}(t)+\mathcal{B}(t), \tag{36}$$

where $\hat{\mathcal{A}}(t)=i\sum_n\int_0^t d\tau[v_1(t-\tau)\hat{R}_n^\dagger(\tau)-u_1(t-\tau)\hat{R}_n(\tau)]$ and $\mathcal{B}(t)=i\sum_n\int_0^t d\tau[v_1(t-\tau)F_{n,\mathrm{eff}}^*(t)-u_1(t-\tau)F_{n,\mathrm{eff}}(t)]$. Comparing Eqs. (33) and (36), we obtain

$$\begin{aligned}
\mu_n(\mathrm{t})&=-ig_n\int_0^t e^{-(i\Delta_n+\frac{\gamma_n}{2})\tau}u_1(t-\tau)d\tau,\\
\nu_n(t)&=ig_n\int_0^t e^{-(-i\Delta_n+\frac{\gamma_n}{2})\tau}v_1(t-\tau)d\tau,\\
\alpha_{nk}(t)&=ig_n\sqrt{\frac{\gamma_n}{2\pi}}\int_0^t d\tau u_1(t-\tau)e^{-(i\Delta_n+\frac{\gamma_n}{2})\tau}\\
&\quad\times\int_0^\tau d\tau_1 e^{[\frac{\gamma_n}{2}-i(\omega_{n,k}-\Omega-\Delta_n)]\tau_1},\\
\beta_{nk}(t)&=-ig_n\sqrt{\frac{\gamma_n}{2\pi}}\int_0^t d\tau v_1(t-\tau)e^{-(-i\Delta_n+\frac{\gamma_n}{2})\tau}\\
&\quad\times\int_0^\tau d\tau_1 e^{[\frac{\gamma_n}{2}+i(\omega_{n,k}-\Omega-\Delta_n)]\tau_1},\\
\eta(t)&=i\sum_n\int_0^t d\tau[v_1(t-\tau)F_{n,\mathrm{eff}}^*(t)-u_1(t-\tau)F_{n,\mathrm{eff}}(t)].
\end{aligned} \tag{37}$$

By solving the coupled equations in Eq. (34), we can obtain the complete information of the quantum network. It is particularly useful in the derivation of the exact non-Markovian master equation for UPB with the non-Markovian effect, which is achieved by integrating out the environmental degrees of freedom (similar to Secs. III and IV). The quantum network with dissipative right cavities and driving fields increases controllabilities for UPB with the non-Markovian effect, which has $n+1$ quantum interference paths shown in Fig. 16.

VIII. CONCLUSION

In summary, we have studied UPB with the non-Markovian effect in a system consisting of the dissipationless left cavity (mediated by two-photon pump) and Markovian dissipative right cavity (driven by single-photon driving field). We derived the exact non-Markovian Heisenberg-Langevin equation and reduced master equation for the left cavity, which contains the two-photon pump and effective single-photon driving field. When the dissipation falls below a threshold, UPB occurs in the non-Markovian regime due to the nonzero effective single-photon driving field. UPB weakens for the left cavity when the dissipation exceeds the threshold in the Markovian regime, and then disappears if the dissipation tends to infinity, which originates from violation of the closed quantum interference paths due to the effective single-photon driving field reaching zero. With the destructive quantum interference effects between different paths for two-photon space, UPB has been analytically found, which is in good agreement with that obtained by the numerical simulation. The existence of dissipations in both cavities is also discussed. Moreover, we extend the results to the system containing a left cavity (mediated by two-photon pump) coupling with noninteracting dissipative right cavities (driven by single-photon driving fields).

The investigations of the left cavity and dissipative right cavity respectively mediated by two-photon pump and single-photon driving field might open a way to better understand the connections between UPB and non-Markovianities, which are available to a variety of physically relevant systems, e.g., (1) second-order nonlinearity $\hat{a}^2\hat{b}^\dagger+\hat{b}\hat{a}^{\dagger 2}$ [49,50], (2) Kerr nonlinear medium $\hat{a}^\dagger\hat{a}^\dagger\hat{a}\hat{a}$ [105,232], (3) Jaynes-Cummings model $\sum_k g_k(\sigma_- b_k^\dagger + b_k\sigma_+)$ [98,233–237] or Rabi model $\sum_k v_k\sigma_x(b_k^\dagger + b_k)$ [238,239], and (4) first-order $\hat{a}^\dagger\hat{a}(\hat{b}+\hat{b}^\dagger)$ [240–242] and (5) quadratic optomechanical couplings $\hat{a}^\dagger\hat{a}(\hat{b}+\hat{b}^\dagger)^2$ [25,243–247], interacting with Markovian environments, which deserve future studies for UPB with non-Markovian effects. As an outlook, how to explore CPB with the non-Markovian effects is still a challenge, which originates from CPB requiring the system to have nonlinearities (linearization methods might be applied to quantum nonlinear systems).

ACKNOWLEDGMENTS

This work was supported by National Natural Science Foundation of China under Grants No. 12175033, and No. 12274064, Natural Science Foundation of Jilin Province (subject arrangement project) under Grant No. 20210101406JC, and Scientific Research Project for Department of Education of Jilin Province under Grant No. JJKH20241410KJ.

APPENDIX A: DEGENERATE OPTICAL PARAMETRIC AMPLIFIER

The two-photon pump can be realized by a degenerate optical parametric amplifier (OPA) in a single cavity containing a $\chi^{(2)}$ nonlinear medium [193–198] given by $\tilde{H}_{\rm OPA} = \omega_c\hat{a}^\dagger\hat{a} + \omega_p\hat{p}^\dagger\hat{p} + J_p(\hat{a}^{\dagger 2}\hat{p} + \hat{p}^\dagger\hat{a}^2)$, where $\hat{a}$ and $\hat{p}$ are the photon annihilation operators of the two cavity modes with frequencies ω_c and ω_p, respectively. J_p denotes the coupling strength via $\chi^{(2)}$ nonlinear medium [248], which mediates the conversion of a photon in cavity p to two photons [13,49,50]. The coupling strength between two cavities is given by

$$J_p = D\varepsilon_0\left(\frac{\hbar\omega_c}{2\varepsilon_0}\right)\sqrt{\frac{\hbar\omega_p}{2\varepsilon_0}}\int d\mathbf{r}\frac{\chi^{(2)}(\mathbf{r})}{[\varepsilon(\mathbf{r})]^3}\alpha_1^2(\mathbf{r})\alpha_2(\mathbf{r}), \quad \text{(A1)}$$

where ε_0 is the vacuum permittivity. $\varepsilon(\mathbf{r})$ denotes the permittivity. D is a degeneracy factor. $\alpha_1(\mathbf{r})$ and $\alpha_2(\mathbf{r})$ are the wave functions for modes $\hat{a}$ and $\hat{p}$, respectively. It is widely recognized that all quantum amplifiers are essentially nonlinear systems [194,248]. As one of the examples of parametric amplification nonlinear interactions, the schematic diagram of the OPA physical process is shown in Fig. 1. The OPA interaction involves a pump photon with frequency ω_p being converted into two photons with identical frequency ω_c with the relation $\omega_p = 2\omega_c$ due to the second-order nonlinearity. The pump is treated approximately as a classical coherent field because the pump depletion is negligible [249–251], namely, $\hat{p} \to \beta e^{-i(\theta_p - \omega_p t)}$ (mean-field approximation, which requires pump amplitude to be very large), with β and θ_p being the amplitude and phase of the pump. With this, the OPA Hamiltonian becomes

$$\hat{H}_{\rm OPA} = \omega_c\hat{a}^\dagger\hat{a} + Ge^{-i\omega_p t}\hat{a}^{\dagger 2} + Ge^{i\omega_p t}\hat{a}^2, \quad \text{(A2)}$$

where $G = J_p\beta e^{-i\theta_p}$ is the nonlinear strength of the OPA with J_p given by Eq. (A1). Obviously, G is proportional to the amplitude of the pump and second-order nonlinearity of the medium.

APPENDIX B: DERIVATION OF EQ. (6)

Substituting $\hat{H}_{\rm eff} = \hat{H}_S - i\gamma\hat{b}^\dagger\hat{b}/2$ [$\hat{H}_S$ is given by Eq. (2)] into Schrödinger equation $i\frac{\partial}{\partial t}|\bar{\psi}\rangle = \hat{H}_{\rm eff}|\bar{\psi}\rangle$, we obtain

$$\begin{aligned}
i\dot{\bar{E}}_{01} &= F\bar{E}_{00} + (\Delta - i\gamma/2)\bar{E}_{01} + g\bar{E}_{10} + \sqrt{2}F^*\bar{E}_{02} = 0,\\
i\dot{\bar{E}}_{10} &= g\bar{E}_{01} + \Delta\bar{E}_{10} + F^*\bar{E}_{11} = 0,\\
i\dot{\bar{E}}_{11} &= F\bar{E}_{10} + (2\Delta - i\gamma/2)\bar{E}_{11} + \sqrt{2}g\bar{E}_{02} + \sqrt{2}g\bar{E}_{20} = 0,\\
i\dot{\bar{E}}_{02} &= \sqrt{2}F\bar{E}_{01} + \sqrt{2}g\bar{E}_{11} + 2(\Delta - i\gamma/2)\bar{E}_{02} = 0,\\
i\dot{\bar{E}}_{20} &= \sqrt{2}G\bar{E}_{00} + \sqrt{2}g\bar{E}_{11} + 2\Delta\bar{E}_{20} = 0.
\end{aligned} \quad \text{(B1)}$$

Under the weak driving condition, we have $|\bar{E}_{00}| \gg |\bar{E}_{10}|, |\bar{E}_{01}| \gg |\bar{E}_{11}|, |\bar{E}_{02}|, |\bar{E}_{20}|$. The condition for $g^{(2)}(0) = \langle\hat{a}^\dagger\hat{a}^\dagger\hat{a}\hat{a}\rangle/\langle\hat{a}^\dagger\hat{a}\rangle^2 \simeq \langle\bar{\psi}|\hat{a}^\dagger\hat{a}^\dagger\hat{a}\hat{a}|\bar{\psi}\rangle/\langle\bar{\psi}|\hat{a}^\dagger\hat{a}|\bar{\psi}\rangle^2 \simeq 2|\bar{E}_{20}|^2/|\bar{E}_{10}|^4 = 0$ is derived from Eq. (B1) by setting $\bar{E}_{20} = 0$. This leads to $-F\bar{E}_{00} = (\Delta - i\gamma/2)\bar{E}_{01} + g\bar{E}_{10}$, $0 = g\bar{E}_{01} + \Delta\bar{E}_{10}$, $0 = F\bar{E}_{10} + (2\Delta - i\gamma/2)\bar{E}_{11} + \sqrt{2}g\bar{E}_{02}$, $0 = F\bar{E}_{01} + g\bar{E}_{11} + \sqrt{2}(\Delta - i\gamma/2)\bar{E}_{02}$, and $0 = G\bar{E}_{00} + g\bar{E}_{11}$. Moreover, we obtain $\bar{E}_{01}/\bar{E}_{10} = -\Delta/g$ and $\bar{E}_{00} = -g\bar{E}_{10}/F - (\Delta - i\gamma/2)\bar{E}_{01}/F$. $\bar{E}_{10}$, $\bar{E}_{11}$, and $\bar{E}_{02}$ having nontrivial solutions require

$$\begin{aligned}
0 = {} & [g^2G - G(\Delta - i\gamma/2)\Delta](2\Delta - i\gamma/2)\\
& \times(\Delta - i\gamma/2) + g^2F^2(\Delta - i\gamma/2) - g^4G\\
& + g^2F^2\Delta + g^2G(\Delta - i\gamma/2)\Delta.
\end{aligned} \quad \text{(B2)}$$

By separating the real and imaginary parts of Eq. (B2), we can get the optimal condition in Eq. (6). The expressions for these coefficients in Eq. (7) are $\bar{m} = 4096G^2$, $\bar{n} = -8192g^2G^2 + 1280G^2k^2 + 256G^2(-16g^2 + 5k^2)$, $\bar{o} = 4096 g^4G^2 - 512g^2G^2k^2 + 64G^2k^4 + 64G^2(4g^2 + k^2)^2 - 512g^2G^2(-16g^2 + 5k^2) + 80G^2k^2(-16g^2 + 5k^2)$, $\bar{p} = -4096f^4g^4 + 256g^4G^2k^2 - 128g^2G^2(4g^2 + k^2)^2 + 20G^2k^2(4g^2 + k^2)^2 + 256g^4G^2(-16g^2 + 5k^2) - 32g^2G^2k^2(-16g^2 + 5k^2) + 4G^2k^4(-16g^2 + 5k^2)$, $\bar{q} = -512f^4g^4k^2 + 64g^4G^2(4g^2 + k^2)^2 - 8g^2G^2k^2(4g^2 + k^2)^2 + G^2k^4(4g^2 + k^2)^2 + 16g^4G^2k^2(-16g^2 + 5k^2)$, and $\bar{r} = -16f^4g^4k^4 + 4g^4G^2k^2(4g^2 + k^2)^2$.

APPENDIX C: DERIVATION OF EQ. (3)

The Heisenberg-Langevin equation [135,252] under the Markovian approximation is written as

$$\begin{aligned}
\frac{d}{dt}\hat{A}(t) = {} & -i[\hat{A}(t), \hat{H}_S(t)] - \frac{\gamma}{2}[\hat{A}(t), \hat{b}^\dagger(t)]\hat{b}(t)\\
& - \sqrt{\gamma}[\hat{A}(t), \hat{b}^\dagger(t)]\hat{e}_{\rm in}(t) + \frac{\gamma}{2}\hat{b}^\dagger(t)[\hat{A}(t), \hat{b}(t)]\\
& + \sqrt{\gamma}\hat{e}_{\rm in}^\dagger(t)[\hat{A}(t), \hat{b}(t)],
\end{aligned} \quad \text{(C1)}$$

where the Heisenberg operator $\hat{A}(t) = e^{i\hat{H}_T t}\hat{A}e^{-i\hat{H}_T t}$ with $\hat{H}_T$ given by Eq. (13), $\hat{e}_{\rm in}(t) = \sum_k e^{-i(\omega_k - \omega_l)t}\hat{e}_k/\sqrt{2\pi}$ with $[\hat{e}_{\rm in}(t), \hat{e}_{\rm in}^\dagger(t')] = \delta(t - t')$, and the total system has been transformed in a rotating frame with the driving frequency ω_l [see Eqs. (2) and (13)]. We take

$$\rho_T(0) = |0\rangle_{aa}\langle 0| \otimes |0\rangle_{bb}\langle 0| \otimes |0\rangle_{EE}\langle 0| \quad \text{(C2)}$$

as an initial state, where $|0\rangle_a$, $|0\rangle_b$, and $|0\rangle_E$ respectively denote the vacuum states of the left cavity, the right cavity, and the Markovian environment, which lead to $\hat{a}|0\rangle_a = 0$, $\hat{b}|0\rangle_b = 0$, and $\hat{e}_k|0\rangle_E = 0$. In this case, we have

$$\frac{d}{dt}\langle\hat{A}(t)\rangle = \mathrm{Tr}\left[\frac{d\hat{A}(t)}{dt}\rho_T(0)\right] \equiv \mathrm{Tr}_S[\hat{A}\dot{\rho}_S(t)] \tag{C3}$$

$$\begin{aligned}&= -i\langle[\hat{A}(t),\hat{H}_S(t)]\rangle - \frac{\gamma}{2}\langle[\hat{A}(t),\hat{b}^\dagger(t)]\hat{b}(t)\rangle\\ &\quad -\sqrt{\gamma}\langle[\hat{A}(t),\hat{b}^\dagger(t)]\hat{e}_{\mathrm{in}}(t)\rangle\\ &\quad +\frac{\gamma}{2}\langle\hat{b}^\dagger(t)[\hat{A}(t),\hat{b}(t)]\rangle\\ &\quad +\sqrt{\gamma}\langle\hat{e}^\dagger_{\mathrm{in}}(t)[\hat{A}(t),\hat{b}(t)]\rangle,\end{aligned} \tag{C4}$$

where $\mathrm{Tr}=\mathrm{Tr}_S\mathrm{Tr}_R$, $\mathrm{Tr}_S=\mathrm{Tr}_a\mathrm{Tr}_b$, $\rho_S(t)=\mathrm{Tr}_R\{\rho_T(t)\}$, and $\rho_T(t)=e^{-i\hat{H}_T t}\rho_T(0)e^{i\hat{H}_T t}$. With $\langle[\hat{A}(t),\hat{b}^\dagger(t)]\hat{e}_{\mathrm{in}}(t)\rangle = \mathrm{Tr}[[\hat{A}(t),\hat{b}^\dagger(t)]\hat{e}_{\mathrm{in}}(t)\rho_T(0)]$ and $\langle\hat{e}^\dagger_{\mathrm{in}}(t)[\hat{A}(t),\hat{b}(t)]\rangle = \mathrm{Tr}\{[\hat{A}(t),\hat{b}(t)]\rho_T(0)\hat{e}^\dagger_{\mathrm{in}}(t)\}$ due to $\hat{e}_{\mathrm{in}}(t)\rho_T(0)=0$ and $\rho_T(0)\hat{e}^\dagger_{\mathrm{in}}(t)=0$, Eq. (C4) becomes

$$\begin{aligned}\frac{d}{dt}\langle\hat{A}(t)\rangle =& -i\mathrm{Tr}\{[\hat{A}(t),\hat{H}_S(t)]\rho_T(0)\}\\ &-\frac{\gamma}{2}\mathrm{Tr}\{[\hat{A}(t),\hat{b}^\dagger(t)]\hat{b}(t)\rho_T(0)\}\\ &+\frac{\gamma}{2}\mathrm{Tr}\{\hat{b}^\dagger(t)[\hat{A}(t),\hat{b}(t)]\rho_T(0)\}\\ =& -i\mathrm{Tr}_S\{[\hat{A},\hat{H}_S]\rho_S(t)\} - \frac{\gamma}{2}\mathrm{Tr}_S\{[\hat{A},\hat{b}^\dagger]\hat{b}\rho_S(t)\}\\ &+\frac{\gamma}{2}\mathrm{Tr}_S\{\hat{b}^\dagger[\hat{A},\hat{b}]\rho_S(t)\}.\end{aligned} \tag{C5}$$

With $\mathrm{Tr}\{[\hat{A},\hat{B}]\hat{C}\}=\mathrm{Tr}\{\hat{A}[\hat{B},\hat{C}]\}$, we get

$$\begin{aligned}\frac{d}{dt}\langle\hat{A}(t)\rangle =& \mathrm{Tr}_S\bigg(\hat{A}\{-i[\hat{H}_S,\rho_S(t)] - \frac{\gamma}{2}[\hat{b}^\dagger,\hat{b}\rho_S(t)]\\ &+\frac{\gamma}{2}[\hat{b},\rho_S(t)\hat{b}^\dagger]\}\bigg).\end{aligned} \tag{C6}$$

Equation (3) can be obtained via Eqs. (C3) and (C6).

APPENDIX D: DERIVATION OF EQ. (19)

Defining $C(t)=v(t)+u(t)$ with $C(0)=1$ and $D(t)=v(t)-u(t)$ with $D(0)=-1$ leads to $\frac{d}{dt}D(t) = -i\Delta D(t)+2iGD^*(t)-\int_0^t d\tau[f(t-\tau)D(\tau)]$. Introducing $M(t)=\frac{1}{2}[D(t)+D^*(t)]$ with $M(0)=-1$ and $N(t)=\frac{1}{2i}[D(t)-D^*(t)]$ with $N(0)=0$, we have

$$\begin{aligned}\frac{d}{dt}M(t) =& \Delta N(t)+2GN(t)-\int_0^t d\tau[M(\tau)f_r(t-\tau)]\\ &-\int_0^t d\tau[N(\tau)f_i(t-\tau)],\\ \frac{d}{dt}N(t) =& -\Delta M(t)+2GM(t)-\int_0^t d\tau[N(\tau)f_r(t-\tau)]\\ &+\int_0^t d\tau[M(\tau)f_i(t-\tau)],\end{aligned} \tag{D1}$$

where $f_r(t)=1/2*[f(t)+f^*(t)]$ and $f_i(t)=i/2*[f(t)-f^*(t)]$. Making the Laplace transformation to Eq. (D1) gives $sM(s)+1=\Delta N(s)+2GN(s)-f_r(s)M(s)-f_i(s)N(s)$ and $sN(s)=-\Delta M(s)+2GM(s)+f_i(s)M(s)-f_r(s)N(s)$, or

$$\begin{aligned}M(s) &= \frac{f_r(s)+s}{-[\Delta-f_i(s)]^2+4G^2-[f_r(s)+s]^2},\\ N(s) &= \frac{\Delta-f_i(s)-2G}{[\Delta-f_i(s)]^2-4G^2+[f_r(s)+s]^2}.\end{aligned} \tag{D2}$$

For $\frac{d}{dt}C(t)=-i\Delta C(t)-2iGC^*(t)-\int_0^t f(t-\tau)C(\tau)d\tau$ and defining $P(t)=\frac{1}{2}[C(t)+C^*(t)]$ with $P(0)=1$ and $Q(t)=\frac{1}{2i}[C(t)-C^*(t)]$ with $Q(0)=0$, we obtain

$$\begin{aligned}\frac{d}{dt}P(t) =& \Delta Q(t)-2GQ(t)-\int_0^t f_i(t-\tau)Q(\tau)d\tau\\ &-\int_0^t f_r(t-\tau)P(\tau)d\tau,\\ \frac{d}{dt}Q(t) =& -\Delta P(t)-2GP(t)+\int_0^t f_i(t-\tau)P(\tau)d\tau\\ &-\int_0^t f_r(t-\tau)Q(\tau)d\tau,\end{aligned} \tag{D3}$$

and $sP(s)-1=\Delta Q(s)-2GQ(s)-f_i(s)Q(s)-f_r(s)P(s)$, $sQ(s)=-\Delta P(s)-2GP(s)+f_i(s)P(s)-f_r(s)Q(s)$, or

$$\begin{aligned}P(s) &= \frac{f_r(s)+s}{[\Delta-f_i(s)]^2-4G^2+[f_r(s)+s]^2},\\ Q(s) &= \frac{\Delta-f_i(s)+2G}{-[\Delta-f_i(s)]^2+4G^2-[f_r(s)+s]^2}.\end{aligned} \tag{D4}$$

Collecting all these together, we get

$$\begin{aligned}u(t) &= \tfrac{1}{2}\{[P(t)-M(t)]+i[Q(t)-N(t)]\},\\ v(t) &= \tfrac{1}{2}\{[P(t)+M(t)]+i[Q(t)+N(t)]\}.\end{aligned} \tag{D5}$$

Moreover, setting $\hat{O}(t)=\frac{1}{2}[\hat{c}(t)+\hat{c}^\dagger(t)]$ with $\hat{O}(0)=0$ and $\hat{B}(t)=\frac{1}{2i}[\hat{c}(t)-\hat{c}^\dagger(t)]$ with $\hat{B}(0)=0$, we obtain

$$\begin{aligned}\frac{d}{dt}\hat{O}(t) =& \Delta\hat{B}(t)-2G\hat{B}(t)\\ &+\frac{i}{2}[F^*_{\mathrm{eff}}(t)-F_{\mathrm{eff}}(t)]+\frac{i}{2}[\hat{R}^\dagger(t)-\hat{R}(t)]\\ &-\int_0^t f_i(t-\tau)\hat{B}(\tau)d\tau-\int_0^t f_r(t-\tau)\hat{O}(\tau)d\tau,\\ \frac{d}{dt}\hat{B}(t) =& -\Delta\hat{O}(t)-2G\hat{O}(t)\\ &-\frac{1}{2}[\hat{R}^\dagger(t)+\hat{R}(t)]-\frac{1}{2}[F^*_{\mathrm{eff}}(t)+F_{\mathrm{eff}}(t)]\\ &-\int_0^t f_r(t-\tau)\hat{B}(\tau)d\tau+\int_0^t f_i(t-\tau)\hat{O}(\tau)d\tau,\end{aligned} \tag{D6}$$

and $s\hat{B}(s)=-\Delta\hat{O}(s)-2G\hat{O}(s)-\frac{1}{2}[\hat{R}(s)+\hat{R}^\dagger(s)]-\frac{1}{2s}[F_{\mathrm{eff}}(s)+F^*_{\mathrm{eff}}(s)]-f_r(s)\hat{B}(s)+f_i(s)\hat{O}(s)$, $s\hat{O}(s)=\Delta\hat{B}(s)-2G\hat{B}(s)+\frac{i}{2}[\hat{R}^\dagger(s)-\hat{R}(s)]+\frac{i}{2s}[F^*_{\mathrm{eff}}(s)-F_{\mathrm{eff}}(s)]-$

$f_i(s)\hat{B}(s) - f_r(s)\hat{O}(s)$, or

$$\hat{O}(s) = \frac{[\hat{R}(s) + F_{\rm eff}(s)/s]\{\Delta - f_i(s) + i[f_r(s) + 2iG + s]\}}{-2\{[\Delta - f_i(s)]^2 - 4G^2 + [f_r(s) + s]^2\}} + \text{H.c.},$$

$$\hat{B}(s) = \frac{i[\hat{R}(s) + F_{\rm eff}(s)/s]\{\Delta - f_i(s) + i[f_r(s) - 2iG + s]\}}{2\{[\Delta - f_i(s)]^2 - 4G^2 + [f_r(s) + s]^2\}} + \text{H.c.}. \tag{D7}$$

With the above results, we have

$$\hat{c}(s) = i[v(s)\hat{R}^\dagger(s) - u(s)\hat{R}(s)] + \beta(s), \tag{D8}$$

with $\beta(s) = i[v(s)F^*_{\rm eff}(s) - u(s)F_{\rm eff}(s)]$. Equation (19) can be obtained by reversing Laplace transformation to Eq. (D8).

APPENDIX E: DERIVATION OF EQ. (20)

The Hamiltonian of the right cavity coupling with the Markovian environment in a rotating frame with the driving frequency ω_l [see Eqs. (2) and (13)],

$$\hat{H}_{be} = \Delta\hat{b}^\dagger\hat{b} + \sum_k(\omega_k - \omega_l)\hat{e}_k^\dagger\hat{e}_k + i\sum_k\sqrt{\frac{\gamma}{2\pi}}(\hat{e}_k^\dagger\hat{b} - \hat{b}^\dagger\hat{e}_k), \tag{E1}$$

can be diagonalized as [253]

$$\hat{H}_{be} = \sum_j \chi_j\hat{B}_j^\dagger\hat{B}_j, \tag{E2}$$

where $\hat{B}_j = \alpha_j\hat{b} + \sum_k\beta_{jk}\hat{e}_k$ meets the bosonic orthogonal-normalization property $[\hat{B}_j, \hat{B}_m^\dagger] = \delta_{jm}$ with

$$\hat{b} = \sum_j\alpha_j^*\hat{B}_j, \quad \hat{e}_k = \sum_j\beta_{jk}^*\hat{B}_j. \tag{E3}$$

Making the commutation relation $[\hat{B}_j, \hat{H}_{be}]$ with Eqs. (E1) and (E2) leads to

$$\chi_j\alpha_j = \Delta\alpha_j + i\sum_k\beta_{jk}\sqrt{\gamma/2\pi},$$
$$\chi_j\beta_{jk} = -i\sqrt{\gamma/2\pi}\alpha_j + \beta_{jk}(\omega_k - \omega_l), \tag{E4}$$

which also satisfy the eigenequation with eigenvalue χ_j and eigenstate $|\varepsilon_j\rangle$ based on Hamiltonian (E1) in single exciton subspace (originating from the total excitation number $\hat{N} = \hat{b}^\dagger\hat{b} + \sum_k\hat{e}_k^\dagger\hat{e}_k$ conserved):

$$\hat{H}_{be}|\varepsilon_j\rangle = \chi_j|\varepsilon_j\rangle, \quad |\varepsilon_j\rangle = \alpha_j|10\rangle + \sum_k\beta_{jk}|01_k\rangle, \tag{E5}$$

where α_j and β_{jk} denote the probability amplitudes on the states $|10\rangle$ and $|01_k\rangle$ with the right cavity and kth mode in the environment respectively having one photon. Substituting Eqs. (E2) and (E3) into Eq. (13), we obtain Eq. (20). In order to compare with Eq. (16), we write down the Heisenberg equation with Eq. (20):

$$\frac{d}{dt}\hat{a} = -i\Delta\hat{a} - 2iG\hat{a}^\dagger - i\sum_j\mu_j^*\hat{B}_j, \tag{E6}$$

$$\frac{d}{dt}\hat{B}_j = -i\chi_j\hat{B}_j - i\mu_j\hat{a} - i\nu_j, \tag{E7}$$

which result in

$$\frac{d}{dt}\hat{a} = -i\Delta\hat{a} - 2iG\hat{a}^\dagger - \int_0^t\tilde{f}(t-\tau)\hat{a}(\tau)d\tau - i\tilde{F}_{\rm eff}(t) - i\tilde{R}(t), \tag{E8}$$

with

$$\tilde{f}(t-\tau) = g^2x(t),$$
$$\tilde{F}_{\rm eff}(t) = -igF\int_0^t x(t-\tau)d\tau,$$
$$\tilde{R}(t) = gx(t)\hat{b} - g\sum_k y_k(t)\hat{e}_k, \tag{E9}$$

where $x(t) = \sum_j|\alpha_j|^2e^{-i\chi_jt}$ and $y_k(t) = \sum_j\alpha_j^*\beta_{jk}e^{-i\chi_jt}$ respectively correspond to the time-dependent probability amplitudes in $|10\rangle$ and $|01_k\rangle$ with Eq. (E1) under the initial state $|\psi(0)\rangle = |10\rangle$ in single exciton subspace proven as follows. Inserting the completeness relation $\sum_j|\varepsilon_j\rangle\langle\varepsilon_j|$ with Eq. (E5) into $|\psi(t)\rangle_{be} = e^{-i\hat{H}_{be}t}|10\rangle$, we obtain

$$|\psi(t)\rangle_{be} = \sum_j|\alpha_j|^2e^{-i\chi_jt}|10\rangle + \sum_{jk}\alpha_j^*\beta_{jk}e^{-i\chi_jt}|01_k\rangle$$
$$\equiv x(t)|10\rangle + \sum_k y_k(t)|01_k\rangle. \tag{E10}$$

The Schrödinger equation $i\partial_t|\psi(t)\rangle_{be} = \hat{H}_{be}|\psi(t)\rangle_{be}$ gives $\dot{x}(t) = -i\Delta x(t) - \sqrt{\gamma/2\pi}\sum_k y_k(t)$ and $\dot{y}_k(t) = -i(\omega_k - \omega_l)y_k(t) + \sqrt{\gamma/2\pi}x(t)$ with $x(0) = 1$ and $y_k(0) = 0$, which lead to $y_k(t) = \sqrt{\gamma/2\pi}\int_0^t e^{-i(\omega_k-\omega_l)(t-\tau)}x(\tau)d\tau$ and $\dot{x} = -i\Delta x(t) - \int_0^t f_1(t-\tau)x(\tau)d\tau$ with $f_1(t-\tau) = \frac{\gamma}{2\pi}\sum_k e^{-i(\omega_k-\omega_l)t} = \gamma\delta(t-\tau)$. With those, we get

$$x(t) = e^{-(i\Delta+\frac{\gamma}{2})t},$$
$$y_k(t) = \sqrt{\gamma/2\pi}\int_0^t e^{-i(\omega_k-\omega_l)(t-\tau)-(i\Delta+\frac{\gamma}{2})\tau}d\tau. \tag{E11}$$

Substituting Eq. (E11) into Eq. (E9), we find that $\tilde{f}(t)$, $\tilde{F}_{\rm eff}(t)$, and $\tilde{R}(t)$ in Eq. (E9) are exactly equal to $f(t)$, $F_{\rm eff}(t)$, and $\hat{R}(t)$ in Eq. (16), respectively.

APPENDIX F: DERIVATION OF EQ. (21)

In the Heisenberg picture with the initial state $\rho_T(0)$ in Eq. (C2) fixed, the time evolution of any physical observable can be obtained directly from Eqs. (17)–(19) through the identity $\text{Tr}[\frac{d\hat{A}_{c_1c_2}(t)}{dt}\rho_T(0)] \equiv \text{Tr}_a[\hat{A}_{c_1c_2}(0)\frac{d\rho(t)}{dt}]$ with $\hat{A}_{c_1c_2}(t) = \hat{a}(t)^{\dagger c_1}\hat{a}(t)^{c_2}$, where $\rho(t) \equiv \text{Tr}_b\rho_S(t)$ given by Eq. (21) denotes the reduced density matrix for the left cavity. $\rho_S(t) = \text{Tr}_{\rm E}\rho_T(t)$ is determined by Eq. (3), where $\rho_T(t) = U(t)\rho_T(0)U^\dagger(t)$ is the density matrix of the total system containing the Markovian environment. $\text{Tr} \equiv \text{Tr}_a\text{Tr}_b\text{Tr}_E$ denotes traces over all the parts of the total system. With Eq. (17), the expectation values $A_{01}(t) = \langle\hat{a}(t)\rangle$, $A_{02}(t) = \langle\hat{a}(t)\hat{a}(t)\rangle$, and $A_{11}(t) = \langle\hat{a}^\dagger(t)\hat{a}(t)\rangle$ are controlled by

$$
\begin{aligned}
\frac{d}{dt}A_{01}(t) &= \varsigma(t)[A_{01}(t)-\beta(t)]+\xi(t)[A_{01}^{*}(t)-\beta^{*}(t)] \\
&\quad +\dot{\beta}(t), \\
\frac{d}{dt}A_{02}(t) &= 2\varsigma(t)A_{02}(t)+2\xi(t)A_{11}(t)+2A_{01}(t)[\dot{\beta}(t) \\
&\quad -\varsigma(t)\beta(t)-\xi(t)\beta^{*}(t)]+\frac{d}{dt}\langle\hat{\alpha}^{2}\rangle-2\varsigma(t)\langle\hat{\alpha}^{2}\rangle \\
&\quad -\xi(t)\langle\hat{\alpha}\hat{\alpha}^{\dagger}+\hat{\alpha}^{\dagger}\hat{\alpha}\rangle+\xi(t), \\
\frac{d}{dt}A_{11}(t) &= \frac{\dot{\vartheta}}{\vartheta}\langle\hat{A}_{11}(t)-\hat{\alpha}^{\dagger}\hat{\alpha}\rangle+\frac{d}{dt}\langle\hat{\alpha}^{\dagger}\hat{\alpha}\rangle+\{\xi^{*}(t)\langle\hat{A}_{02}(t) \\
&\quad -\hat{\alpha}^{2}\rangle+A_{01}^{*}(t)[\dot{\beta}(t)-\varsigma(t)\beta(t)-\xi(t)\beta^{*}(t)] \\
&\quad +\text{H.c.}\},
\end{aligned}
\tag{F1}
$$

with $\varsigma(t)=(\dot{u}u^{*}-\dot{v}v^{*})/\vartheta(t)$, $\xi(t)=(u\dot{v}-\dot{u}v)/\vartheta(t)$, and $\vartheta(t)=|u(t)|^{2}-|v(t)|^{2}$, where $u(t)$ and $v(t)$ are determined by Eq. (18).

To give the time coefficients in Eq. (21), we compute

$$
\begin{aligned}
\frac{d}{dt}A_{01}(t) &= -\left[\frac{1}{2}\kappa_{1}(t)+iX(t)\right]A_{01}(t)-2iY(t)A_{01}^{*}(t)-iZ(t), \\
\frac{d}{dt}A_{02}(t) &= -4iY(t)A_{11}(t)-[\kappa_{1}(t)+2iX(t)]A_{02}(t) \\
&\quad -[\kappa_{3}(t)+2iY(t)]-2iZ(t)A_{01}(t), \\
\frac{d}{dt}A_{11}(t) &= \frac{1}{2}\kappa_{2}(t)-\kappa_{1}(t)A_{11}(t)+\{2iY^{*}(t)A_{02}(t) \\
&\quad +iZ^{*}(t)A_{01}(t)+\text{H.c.}\}.
\end{aligned}
\tag{F2}
$$

By comparing Eqs. (F1) and (F2), we get

$$
\begin{aligned}
&Y(t)=-\xi(t)/2i, \\
&X(t)=-\mathrm{Im}[\varsigma(t)], \\
&Z(t)=i[\dot{\beta}(t)-\varsigma(t)\beta(t)-\xi(t)\beta^{*}(t)], \\
&\kappa_{1}(t)=-\dot{\vartheta}(t)/\vartheta(t), \\
&\kappa_{2}(t)=2[\partial/\partial t+\kappa_{1}(t)]\langle\hat{\alpha}^{\dagger}\hat{\alpha}\rangle-2\{\xi^{*}(t)\langle\hat{\alpha}^{2}\rangle+\text{H.c.}\}, \\
&\kappa_{3}(t)=[2\varsigma(t)-\partial/\partial t]\langle\hat{\alpha}^{2}\rangle+\xi(t)\langle\hat{\alpha}\hat{\alpha}^{\dagger}+\hat{\alpha}^{\dagger}\hat{\alpha}\rangle.
\end{aligned}
\tag{F3}
$$

[1] A. Imamoğlu, H. Schmidt, G. Woods, and M. Deutsch, Strongly interacting photons in a nonlinear cavity, Phys. Rev. Lett. **79**, 1467 (1997).

[2] B. Dayan, A. S. Parkins, T. Aoki, E. P. Ostby, K. J. Vahala, and H. J. Kimble, A photon turnstile dynamically regulated by one atom, Science **319**, 1062 (2008).

[3] J. S. Tang, L. Tang, H. D. Wu, Y. Wu, H. Sun, H. Zhang, T. Li, Y. Q. Lu, M. Xiao, and K. Y. Xia, Towards on-demand heralded single-photon sources via photon blockade, Phys. Rev. Appl. **15**, 064020 (2021).

[4] A. J. Shields, Semiconductor quantum light sources, Nat. Photonics. **1**, 215 (2007).

[5] L. Davidovich, Sub-Poissonian processes in quantum optics, Rev. Mod. Phys. **68**, 127 (1996).

[6] K. M. Birnbaum, A. Boca, R. Miller, A. D. Boozer, T. E. Northup, and H. J. Kimble, Photon blockade in an optical cavity with one trapped atom, Nature (London) **436**, 87 (2005).

[7] A. Faraon, I. Fushman, D. Englund, N. Stoltz, P. Petroff, and J. Vučković, Coherent generation of non-classical light on a chip via photon-induced tunnelling and blockade, Nat. Phys. **4**, 859 (2008).

[8] L. Tian and H. J. Carmichael, Quantum trajectory simulations of two-state behavior in an optical cavity containing one atom, Phys. Rev. A **46**, R6801(R) (1992).

[9] M. J. Werner and A. Imamoğlu, Photon-photon interactions in cavity electromagnetically induced transparency, Phys. Rev. A **61**, 011801(R) (1999).

[10] R. J. Brecha, P. R. Rice, and M. Xiao, N two-level atoms in a driven optical cavity: Quantum dynamics of forward photon scattering for weak incident fields, Phys. Rev. A **59**, 2392 (1999).

[11] S. Rebic, S. M. Tan, A. S. Parkins, and D. F. Walls, Large Kerr nonlinearity with a single atom, J. Opt. B **1**, 490 (1999).

[12] X. Y. Liang, Z. L. Duan, Q. Guo, C. J. Liu, S. G. Guan, and Y. Ren, Antibunching effect of photons in a two-level emitter-cavity system, Phys. Rev. A **100**, 063834 (2019).

[13] Y. Y. Yan, Y. B. Cheng, S. G. Guan, D. Y. Yu, and Z. L. Duan, Pulse-regulated single-photon generation via quantum interference in a $\chi^{(2)}$ nonlinear nanocavity, Opt. Lett. **43**, 5086 (2018).

[14] J. M. Fink, A. Dombi, A. Vukics, A. Wallraff, and P. Domokos, Observation of the photon-blockade breakdown phase transition, Phys. Rev. X **7**, 011012 (2017).

[15] C. L. Zhai, R. Huang, B. J. Li, H. Jing, and L. M. Kuang, Mechanical engineering of photon blockades in a cavity optomechanical system, arXiv:1901.07654.

[16] K. Hou, C. J. Zhu, Y. P. Yang, and G. S. Agarwal, Interfering pathways for photon blockade in cavity QED with one and two qubits, Phys. Rev. A **100**, 063817 (2019).

[17] M. Leib, F. Deppe, A. Marx, R. Gross, and M. J. Hartmann, Networks of nonlinear superconducting transmission line resonators, New J. Phys. **14**, 075024 (2012).

[18] M. Leib and M. J. Hartmann, Bose-Hubbard dynamics of polaritons in a chain of circuit quantum electrodynamics cavities, New J. Phys. **12**, 093031 (2010).

[19] J. Kim, O. Bensen, H. Kan, and Y. Yamamoto, A single-photon turnstile device, Nature (London) **397**, 500 (1999) I. I. Smolyaninov, A. V. Zayats, A. Gungor, and C. C. Davis, Single-photon tunneling via localized surface plasmons, Phys. Rev. Lett. **88**, 187402 (2002); S. Rebić, A. S. Parkins, and S. M. Tan, Photon statistics of a single-atom intracavity system involving electromagnetically induced transparency, Phys. Rev. A **65**, 063804 (2002); D. G. Angelakis, M. F. Santos, and S. Bose, Photon-blockade-induced Mott transitions and XY spin models in coupled cavity arrays, *ibid.* **76**, 031805(R) (2007); Y. X. Liu, X. W. Xu, A. Miranowicz, and F. Nori, From

blockade to transparency: Controllable photon transmission through a circuit-QED system, *ibid.* **89**, 043818 (2014); A. Faraon, A. Majumdar, and J. Vučković, Generation of nonclassical states of light via photon blockade in optical nanocavities, *ibid.* **81**, 033838 (2010).
[20] A. J. Hoffman, S. J. Srinivasan, S. Schmidt, L. Spietz, J. Aumentado, H. E. Türeci, and A. A. Houck, Dispersive photon blockade in a superconducting circuit, Phys. Rev. Lett. **107**, 053602 (2011).
[21] C. Lang, D. Bozyigit, C. Eichler, L. Steffen, J. M. Fink, A. A. Abdumalikov, Jr., M. Baur, S. Filipp, M. P. da Silva, A. Blais, and A. Wallraff, Observation of resonant photon blockade at microwave frequencies using correlation function measurements, Phys. Rev. Lett. **106**, 243601 (2011).
[22] P. Rabl, Photon blockade effect in optomechanical systems, Phys. Rev. Lett. **107**, 063601 (2011).
[23] A. Nunnenkamp, K. Børkje, and S. M. Girvin, Single-photon optomechanics, Phys. Rev. Lett. **107**, 063602 (2011); C. Shang, Coupling enhancement and symmetrization of single-photon optomechanics in open quantum systems, arXiv:2302.04897.
[24] J. Q. Liao and C. K. Law, Correlated two-photon transport in a one-dimensional waveguide side-coupled to a nonlinear cavity, Phys. Rev. A **82**, 053836 (2010).
[25] J. Q. Liao and F. Nori, Photon blockade in quadratically coupled optomechanical systems, Phys. Rev. A **88**, 023853 (2013).
[26] X. Y. Lü, Y. Wu, J. R. Johansson, H. Jing, J. Zhang, and F. Nori, Squeezed optomechanics with phase-matched amplification and dissipation, Phys. Rev. Lett. **114**, 093602 (2015).
[27] P. Kómár, S. D. Bennett, K. Stannigel, S. J. M. Habraken, P. Rabl, P. Zoller, and M. D. Lukin, Single-photon nonlinearities in two-mode optomechanics, Phys. Rev. A **87**, 013839 (2013).
[28] X. Y. Lü, W. M. Zhang, S. Ashhab, Y. Wu, and F. Nori, Quantum-criticality-induced strong Kerr nonlinearities in optomechanical systems, Sci. Rep. **3**, 2943 (2013).
[29] X. N. Xu, M. Gullans, and J. M. Taylor, Quantum nonlinear optics near optomechanical instabilities, Phys. Rev. A **91**, 013818 (2015).
[30] H. Xie, G. W. Lin, X. Chen, Z. H. Chen, and X. M. Lin, Single-photon nonlinearities in a strongly driven optomechanical system with quadratic coupling, Phys. Rev. A **93**, 063860 (2016).
[31] H. Xie, C. G. Liao, X. Shang, M. Y. Ye, and X. M. Lin, Phonon blockade in a quadratically coupled optomechanical system, Phys. Rev. A **96**, 013861 (2017).
[32] H. Wang, X. Gu, Y. X. Liu, A. Miranowicz, and F. Nori, Tunable photon blockade in a hybrid system consisting of an optomechanical device coupled to a two-level system, Phys. Rev. A **92**, 033806 (2015).
[33] F. Zou, L. B. Fan, J. F. Huang, and J. Q. Liao, Enhancement of few-photon optomechanical effects with cross-Kerr nonlinearity, Phys. Rev. A **99**, 043837 (2019).
[34] Y. X. Liu, A. Miranowicz, Y. B. Gao, J. Bajer, C. P. Sun, and F. Nori, Qubit-induced phonon blockade as a signature of quantum behavior in nanomechanical resonators, Phys. Rev. A **82**, 032101 (2010).
[35] Y. Qu, J. H. Li, and Y. Wu, Interference-modulated photon statistics in whispering-gallery-mode microresonator optomechanics, Phys. Rev. A **99**, 043823 (2019).
[36] J. C. López Carreño, C. Sánchez Muñoz, D. Sanvitto, E. del Valle, and F. P. Laussy, Exciting polaritons with quantum light, Phys. Rev. Lett. **115**, 196402 (2015).
[37] T. Grujic, S. R. Clark, D. Jaksch, and D. G. Angelakis, Non-equilibrium many-body effects in driven nonlinear resonator arrays, New J. Phys. **14**, 103025 (2012).
[38] A. Le Boité, M. J. Hwang, H. Nha, and M. B. Plenio, Fate of photon blockade in the deep strong-coupling regime, Phys. Rev. A **94**, 033827 (2016).
[39] A. Ridolfo, M. Leib, S. Savasta, and M. J. Hartmann, Photon blockade in the ultrastrong coupling regime, Phys. Rev. Lett. **109**, 193602 (2012).
[40] M. Radulaski, K. A. Fischer, K. G. Lagoudakis, J. L. Zhang, and J. Vučković, Photon blockade in two-emitter-cavity systems, Phys. Rev. A **96**, 011801(R) (2017).
[41] H. L. Zhang and Z. L. Duan, Photon blockade in the Jaynes-Cummings model with two-photon dissipation, Opt. Express **31**, 22580 (2023).
[42] Y. T. Guo, F. Zou, J. F. Huang, and J. Q. Liao, Retrieval of photon blockade effect in the dispersive Jaynes-Cummings model, Phys. Rev. A **105**, 013705 (2022).
[43] Z. G. Li, X. M. Li, and X. L. Zhong, Strong photon blockade in an all-fiber emitter-cavity quantum electrodynamics system, Phys. Rev. A **103**, 043724 (2021).
[44] C. S. Zhao, X. Li, S. L. Chao, R. Peng, C. Li, and L. Zhou, Simultaneous blockade of a photon, phonon, and magnon induced by a two-level atom, Phys. Rev. A **101**, 063838 (2020).
[45] S. Ghosh and T. C. H. Liew, Dynamical blockade in a single-mode bosonic system, Phys. Rev. Lett. **123**, 013602 (2019).
[46] A. P. Foster, D. Hallett, I. V. Iorsh, S. J. Sheldon, M. R. Godsland, B. Royall, E. Clarke, I. A. Shelykh, A. M. Fox, M. S. Skolnick, I. E. Itskevich, and L. R. Wilson, Tunable photon statistics exploiting the fano effect in a waveguide, Phys. Rev. Lett. **122**, 173603 (2019).
[47] M. Bajcsy, A. Majumdar, A. Rundquist, and J. Vučković, Photon blockade with a four-level quantum emitter coupled to a photonic-crystal nanocavity, New J. Phys. **15**, 025014 (2013).
[48] Y. Ren, S. H. Duan, W. Z. Xie, Y. K. Shao, and Z. L. Duan, Antibunched photon-pair source based on photon blockade in a nondegenerate optical parametric oscillator, Phys. Rev. A **103**, 053710 (2021).
[49] A. Majumdar and D. Gerace, Single-photon blockade in doubly resonant nanocavities with second-order nonlinearity, Phys. Rev. B **87**, 235319 (2013).
[50] H. Z. Shen, Y. H. Zhou, and X. X. Yi, Quantum optical diode with semiconductor microcavities, Phys. Rev. A **90**, 023849 (2014).
[51] T. E. Lee and M. C. Cross, Quantum-classical transition of correlations of two coupled cavities, Phys. Rev. A **88**, 013834 (2013).
[52] Y. H. Zhou, X. Y. Zhang, T. Liu, Q. C. Wu, Z. C. Shi, H. Z. Shen, and C. P. Yang, Environmentally induced photon blockade via two-photon absorption, Phys. Rev. Appl. **18**, 064009 (2022).
[53] D. Roberts and A. A. Clerk, Driven-dissipative quantum kerr resonators: New exact solutions, photon blockade and quantum bistability, Phys. Rev. X **10**, 021022 (2020).

[54] F. Zou, D. G. Lai, and J. Q. Liao, Enhancement of photon blockade effect via quantum interference, Opt. Express **28**, 16175 (2020).

[55] D. Gerace, H. E. Türeci, A. Imamoglu, V. Giovannetti, and R. Fazio, The quantum-optical Josephson interferometer, Nat. Phys. **5**, 281 (2009).

[56] F. Fratini, E. Mascarenhas, L. Safari, J.-Ph. Poizat, D. Valente, A. Auffèves, D. Gerace, and M. F. Santos, Fabry-perot interferometer with quantum mirrors: Nonlinear light transport and rectification, Phys. Rev. Lett. **113**, 243601 (2014); C. Shang, H. Z. Shen, and X. X. Yi, Nonreciprocity in a strongly coupled three-mode optomechanical circulatory system, Opt. Express **27**, 25882 (2019).

[57] E. Mascarenhas, D. Gerace, D. Valente, S. Montangero, A. Auffèves, and M. F. Santos, A quantum optical valve in a nonlinear-linear resonators junction, Europhys. Lett. **106**, 54003 (2014).

[58] D. E. Chang, A. S. Sørensen, E. A. Demler, and M. D. Lukin, A single-photon transistor using nanoscale surface plasmons, Nat. Phys. **3**, 807 (2007).

[59] R. Huang, Ş. K. Özdemir, J. Q. Liao, F. Minganti, L. M. Kuang, F. Nori, and H. Jing, Exceptional photon blockade: Engineering photon blockade with chiral exceptional points, Laser Photon. Rev. **16**, 2100430 (2022).

[60] J. Y. Sun and H. Z. Shen, Photon blockade in non-Hermitian optomechanical systems with nonreciprocal couplings, Phys. Rev. A **107**, 043715 (2023).

[61] K. Wang, H. Wang, Y. P. Gao, D. Q. Yang, R. Z. Jiao, and C. Wang, Unconventional photon blockade in a non-Hermitian indirectly coupled resonator system, Opt. Express **31**, 1629 (2023).

[62] Y. H. Zhou, H. Z. Shen, X. Y. Zhang, and X. X. Yi, Zero eigenvalues of a photon blockade induced by a non-Hermitian Hamiltonian with a gain cavity, Phys. Rev. A **97**, 043819 (2018).

[63] A. Ben-Asher, A. I. Fernández-Domínguez, and J. Feist, Non-hermitian anharmonicity induces single-photon emission, Phys. Rev. Lett. **130**, 243601 (2023).

[64] D. Y. Wang, C. H. Bai, S. T. Liu, S. Zhang, and H. F. Wang, Distinguishing photon blockade in a $\mathcal{PT}$-symmetric optomechanical system, Phys. Rev. A **99**, 043818 (2019).

[65] D. Y. Wang, C. H. Bai, S. T. Liu, S. Zhang, and H. F. Wang, Photon blockade in a double-cavity optomechanical system with nonreciprocal coupling, New J. Phys. **22**, 093006 (2020).

[66] Y. L. Zuo, R. Huang, L. M. Kuang, X. W. Xu, and H. Jing, Loss-induced suppression, revival, and switch of photon blockade, Phys. Rev. A **106**, 043715 (2022).

[67] J. Zhang, B. Peng, Ş. K. Özdemir, Y. X. Liu, H. Jing, X. Y. Lü, Y. L. Liu, L. Yang, and F. Nori, Giant nonlinearity via breaking parity-time symmetry: A route to low-threshold phonon diodes, Phys. Rev. B **92**, 115407 (2015).

[68] J. H. Li, R. Yu, and Y. Wu, Proposal for enhanced photon blockade in parity-time-symmetric coupled microcavities, Phys. Rev. A **92**, 053837 (2015).

[69] H. Xie, L. W. He, X. Shang, G. W. Lin, and X. M. Lin, Nonreciprocal photon blockade in cavity optomagnonics, Phys. Rev. A **106**, 053707 (2022).

[70] R. Huang, A. Miranowicz, J.-Q. Liao, F. Nori, and H. Jing, Nonreciprocal photon blockade, Phys. Rev. Lett. **121**, 153601 (2018).

[71] W. S. Xue, H. Z. Shen, and X. X. Yi, Nonreciprocal conventional photon blockade in driven dissipative atom-cavity, Opt. Lett. **45**, 4424 (2020).

[72] K. Wang, Q. Wu, Y. F. Yu, and Z. M. Zhang, Nonreciprocal photon blockade in a two-mode cavity with a second-order nonlinearity, Phys. Rev. A **100**, 053832 (2019).

[73] Y. M. Liu, J. Cheng, H. F. Wang, and X. X. Yi, Simultaneous nonreciprocal conventional photon blockades of two independent optical modes by a two-level system, Phys. Rev. A **107**, 063701 (2023).

[74] X. Y. Yao, H. Ali, F. L. Li, and P. B. Li, Nonreciprocal phonon blockade in a spinning acoustic ring cavity coupled to a two-level system, Phys. Rev. Appl. **17**, 054004 (2022).

[75] Y. W. Jing, H. Q. Shi, and X. W. Xu, Nonreciprocal photon blockade and directional amplification in a spinning resonator coupled to a two-level atom, Phys. Rev. A **104**, 033707 (2021).

[76] A. Miranowicz, J. Bajer, N. Lambert, Y. X. Liu, and F. Nori, Tunable multiphonon blockade in coupled nanomechanical resonators, Phys. Rev. A **93**, 013808 (2016).

[77] J. Z. Lin, K. Hou, C. J. Zhu, and Y. P. Yang, Manipulation and improvement of multiphoton blockade in a cavity-QED system with two cascade three-level atoms, Phys. Rev. A **99**, 053850 (2019).

[78] C. J. Zhu, Y. P. Yang, and G. S. Agarwal, Collective multiphoton blockade in cavity quantum electrodynamics, Phys. Rev. A **95**, 063842 (2017).

[79] A. Miranowicz, M. Paprzycka, Y. X. Liu, J. Bajer, and F. Nori, Two-photon and three-photon blockades in driven nonlinear systems, Phys. Rev. A **87**, 023809 (2013); Y. C. Li, Z. H. Yao, and H. Yang, One-photon andtwo-photon blockades in a four-wave-mixing system embedded with an atom, *ibid.* **109**, 043702 (2024).

[80] C. Hamsen, K. N. Tolazzi, T. Wilk, and G. Rempe, Two-photon blockade in an atom-driven cavity QED system, Phys. Rev. Lett. **118**, 133604 (2017).

[81] Z. Haider, S. Qamar, and M. Irfan, Multiphoton blockade and antibunching in an optical cavity coupled with dipole-dipole-interacting Λ-type atoms, Phys. Rev. A **107**, 043702 (2023).

[82] F. Zou, X. Y. Zhang, X. W. Xu, J. F. Huang, and J. Q. Liao, Multiphoton blockade in the two-photon Jaynes-Cummings model, Phys. Rev. A **102**, 053710 (2020).

[83] G. H. Hovsepyan, A. R. Shahinyan, and G. Y. Kryuchkyan, Multiphoton blockades in pulsed regimes beyond stationary limits, Phys. Rev. A **90**, 013839 (2014).

[84] A. Kowalewska-Kudłaszyk, S. I. Abo, G. Chimczak, J. Peřina, Jr., F. Nori, and A. Miranowicz, Two-photon blockade and photon-induced tunneling generated by squeezing, Phys. Rev. A **100**, 053857 (2019).

[85] L. J. Feng and S. Q. Gong, Two-photon blockade generated and enhanced by mechanical squeezing, Phys. Rev. A **103**, 043509 (2021).

[86] Q. Bin, X. Y. Lü, S. W. Bin, and Y. Wu, Two-photon blockade in a cascaded cavity-quantum-electrodynamics system, Phys. Rev. A **98**, 043858 (2018).

[87] W. W. Deng, G. X. Li, and H. Qin, Enhancement of the two-photon blockade in a strong-coupling qubit-cavity system, Phys. Rev. A **91**, 043831 (2015).

[88] T. C. H. Liew and V. Savona, Single photons from coupled quantum modes, Phys. Rev. Lett. **104**, 183601 (2010).

[89] M. Bamba, A. Imamoğlu, I. Carusotto, and C. Ciuti, Origin of strong photon antibunching in weakly nonlinear photonic molecules, Phys. Rev. A **83**, 021802(R) (2011).

[90] H. Flayac and V. Savona, Unconventional photon blockade, Phys. Rev. A **96**, 053810 (2017).

[91] E. Z. Casalengua, J. C. L. Carreño, F. P. Laussy, and E. del Valle, Conventional and unconventional photon statistics, Laser Photon. Rev. **14**, 1900279 (2020).

[92] X. W. Xu and Y. Li, Tunable photon statistics in weakly nonlinear photonic molecules, Phys. Rev. A **90**, 043822 (2014).

[93] I. Carusotto and C. Ciuti, Quantum fluids of light, Rev. Mod. Phys. **85**, 299 (2013); X. W. Xu and Y. Li, Strongly correlated two-photon transport in a one-dimensional waveguide coupled to a weakly nonlinear cavity, Phys. Rev. A **90**, 033832 (2014); J. T. Shen and S. H. Fan, Strongly correlated two-photon transport in a one-dimensional waveguide coupled to a two-level system, Phys. Rev. Lett. **98**, 153003 (2007); X. W. Xu and Y. Li, Strong photon antibunching of symmetric and antisymmetric modes in weakly nonlinear photonic molecules, Phys. Rev. A **90**, 033809 (2014); T. C. H. Liew and V. Savona, Multimode entanglement in coupled cavity arrays, New J. Phys. **15**, 025015 (2013).

[94] H. J. Carmichael, Photon antibunching and squeezing for a single atom in a resonant cavity, Phys. Rev. Lett. **55**, 2790 (1985).

[95] M. Bamba and C. Ciuti, Counter-polarized single-photon generation from the auxiliary cavity of a weakly nonlinear photonic molecule, Appl. Phys. Lett. **99**, 171111 (2011); O. Kyriienko, I. A. Shelykh, and T. C. H. Liew, Tunable single-photon emission from dipolaritons, Phys. Rev. A **90**, 033807 (2014); T. C. H. Liew and V. Savona, Quantum entanglement in nanocavity arrays, *ibid.* **85**, 050301(R) (2012).

[96] A. Majumdar, M. Bajcsy, A. Rundquist, and J. Vučković, Loss-enabled sub-Poissonian light generation in a bimodal nanocavity, Phys. Rev. Lett. **108**, 183601 (2012).

[97] W. Zhang, Z. Y. Yu, Y. M. Liu, and Y. W. Peng, Optimal photon antibunching in a quantum-dot-bimodal-cavity system, Phys. Rev. A **89**, 043832 (2014).

[98] J. Tang, W. D. Geng, and X. L. Xu, Quantum interference induced photon blockade in a coupled single quantum dot-cavity system, Sci. Rep. **5**, 9252 (2015).

[99] H. Jabri and H. Eleuch, Enhanced unconventional photon-blockade effect in one- and two-qubit cavities interacting with nonclassical light, Phys. Rev. A **106**, 023704 (2022).

[100] Y. Wang, W. Verstraelen, B. Zhang, T. C. H. Liew, and Y. D. Chong, Giant enhancement of unconventional photon blockade in a dimer chain, Phys. Rev. Lett. **127**, 240402 (2021).

[101] X. Y. Liang, Z. L. Duan, Q. Guo, S. G. Guan, M. Xie, and C. J. Liu, Photon blockade in a bimode nonlinear nanocavity embedded with a quantum dot, Phys. Rev. A **102**, 053713 (2020).

[102] J. Tang, Y. G. Deng, and C. H. Lee, Strong photon blockade mediated by optical stark shift in a single-atom-cavity system, Phys. Rev. Appl. **12**, 044065 (2019).

[103] J. H. Li and Y. Wu, Quality of photon antibunching in two cavity-waveguide arrangements on a chip, Phys. Rev. A **98**, 053801 (2018).

[104] H. Flayac and V. Savona, Single photons from dissipation in coupled cavities, Phys. Rev. A **94**, 013815 (2016).

[105] H. Z. Shen, Y. H. Zhou, and X. X. Yi, Tunable photon blockade in coupled semiconductor cavities, Phys. Rev. A **91**, 063808 (2015).

[106] H. Flayac, D. Gerace, and V. Savona, An all-silicon single-photon source by unconventional photon blockade, Sci. Rep. **5**, 11223 (2015).

[107] H. Z. Shen, Y. H. Zhou, H. D. Liu, G. C. Wang, and X. X. Yi, Exact optimal control of photon blockade with weakly nonlinear coupled cavities, Opt. Express **23**, 32835 (2015).

[108] Y. H. Zhou, H. Z. Shen, and X. X. Yi, Unconventional photon blockade with second-order nonlinearity, Phys. Rev. A **92**, 023838 (2015).

[109] H. Z. Shen, S. Xu, Y. H. Zhou, G. C. Wang, and X. X. Yi, Unconventional photon blockade from bimodal driving and dissipations in coupled semiconductor microcavities, J. Phys. B **51**, 035503 (2018).

[110] Y. H. Zhou, H. Z. Shen, X. Q. Shao, and X. X. Yi, Strong photon antibunching with weak second-order nonlinearity under dissipation and coherent driving, Opt. Express **24**, 17332 (2016).

[111] H. Flayac and V. Savona, Input-output theory of the unconventional photon blockade, Phys. Rev. A **88**, 033836 (2013); D. Gerace and V. Savona, Unconventional photon blockade in doubly resonant microcavities with second-order nonlinearity, *ibid.* **89**, 031803(R) (2014); S. Ferretti, V. Savona, and D. Gerace, Optimal antibunching in passive photonic devices based on coupled nonlinear resonators, New J. Phys. **15**, 025012 (2013).

[112] O. Kyriienko and T. C. H. Liew, Triggered single-photon emitters based on stimulated parametric scattering in weakly nonlinear systems, Phys. Rev. A **90**, 063805 (2014).

[113] M. Li, Y. L. Zhang, S. H. Wu, C. H. Dong, X. B. Zou, G. C. Guo, and C. L. Zou, Single-mode photon blockade enhanced by Bi-Tone drive, Phys. Rev. Lett. **129**, 043601 (2022).

[114] W. Z. Xie, Q. Guo, and Z. L. Duan, Phonon blockade in an acoustic cavity coupled to a three-level artificial atom, Phys. Rev. B **106**, 115435 (2022).

[115] J. H. Li, C. L. Ding, and Y. Wu, Enhanced photon antibunching via interference effects in a Δ configuration, Phys. Rev. A **100**, 033814 (2019).

[116] Q. H. Liu, G. C. Wang, T. Z. Luan, and H. Z. Shen, Atom mediated single-photon nonlinearity in a quadratically coupled optomechanical system, Adv. Quantum Technol. **7**, 2300422 (2024); X. W. Xu and Y. J. Li, Antibunching photons in a cavity coupled to an optomechanical system, J. Phys. B **46**, 035502 (2013).

[117] V. Savona, Unconventional photon blockade in coupled optomechanical systems, arXiv:1302.5937.

[118] B. Sarma and A. K. Sarma, Unconventional photon blockade in three-mode optomechanics, Phys. Rev. A **98**, 013826 (2018).

[119] S. Dufferwiel, F. Fras, A. Trichet, P. M. Walker, F. Li, L. Giriunas, M. N. Makhonin, L. R. Wilson, J. M. Smith, E. Clarke, M. S. Skolnick, and D. N. Krizhanovskii, Strong exciton-photon coupling in open semiconductor microcavities, Appl. Phys. Lett. **104**, 192107 (2014).

[120] M. A. Lemonde, N. Didier, and A. A. Clerk, Antibunching and unconventional photon blockade with Gaussian squeezed states, Phys. Rev. A **90**, 063824 (2014).

[121] H. Z. Shen, C. Shang, Y. H. Zhou, and X. X. Yi, Unconventional single-photon blockade in non-Markovian systems, Phys. Rev. A **98**, 023856 (2018).

[122] B. Sarma and A. K. Sarma, Quantum-interference-assisted photon blockade in a cavity via parametric interactions, Phys. Rev. A **96**, 053827 (2017); H. Y. Sun, C. Shang, X. X. Luo, Y. H. Zhou, and H. Z. Shen, Optical-assisted photon blockade in a cavity system via parametric interactions, Int. J. Theor. Phys. **58**, 3640 (2019).

[123] B. J. Li, R. Huang, X. W. Xu, A. Miranowicz, and H. Jing, Nonreciprocal unconventional photon blockade in a spinning optomechanical system, Photon. Res. **7**, 630 (2019).

[124] Y. M. Liu, J. Cheng, H. F. Wang, and X. X. Yi, Nonreciprocal photon blockade in a spinning optomechanical system with nonreciprocal coupling, Opt. Express **31**, 12847 (2023).

[125] J. Wang, Q. Wang, and H. Z. Shen, Nonreciprocal unconventional photon blockade with spinning atom-cavity, Europhys. Lett. **134**, 64003 (2021); T. Z. Luan, J. X. Yang, J. Wang, H. Z. Shen, Y. H. Zhou, and X. X. Yi, Nonreciprocal unconventional photon blockade with spinning two-mode cavity coupled via $\chi^{(2)}$ nonlinearities, Int. J. Quantum Inform. **21**, 2350021 (2023).

[126] H. Z. Shen, T. Z. Luan, Y. H. Zhou, Z. C. Shi, and X. X. Yi, Nonreciprocal unconventional photon blockade in atom-cavity with $\chi^{(2)}$ nonlinear medium, Int. J. Quantum Inform. **21**, 2350029 (2023); D. Y. Wang, L. L. Yan, S. L. Su, C. H. Bai, H. F. Wang, and E. J. Liang, Squeezing-induced nonreciprocal photon blockade in an optomechanical microresonator, Opt. Express **31**, 22343 (2023).

[127] Y. M. Wang, W. Xiong, Z. Y. Xu, G. Q. Zhang, and J. Q. You, Dissipation-induced nonreciprocal magnon blockade in a magnon-based hybrid system, Sci. China Phys. Mech. Astron. **65**, 260314 (2022).

[128] H. Z. Shen, Q. Wang, J. Wang, and X. X. Yi, Nonreciprocal unconventional photon blockade in a driven dissipative cavity with parametric amplification, Phys. Rev. A **101**, 013826 (2020).

[129] X. W. Xia, X. Q. Zhang, J. P. Xu, H. Z. Li, Z. Y. Fu, and Y. P. Yang, Giant nonreciprocal unconventional photon blockade with a single atom in an asymmetric cavity, Phys. Rev. A **104**, 063713 (2021).

[130] W. Zhang, T. Wang, S. T. Liu, S. Zhang, and H. F. Wang, Nonreciprocal photon blockade in a spinning resonator coupled to two two-level atoms, Sci. China Phys. Mech. Astron. **66**, 240313 (2023).

[131] X. W. Xia, X. Q. Zhang, J. P. Xu, H. Z. Li, Z. Y. Fu, and Y. P. Yang, Improvement of nonreciprocal unconventional photon blockade by two asymmetrical arranged atoms embedded in a cavity, Opt. Express **30**, 7907 (2022).

[132] C. Vaneph, A. Morvan, G. Aiello, M. Féchant, M. Aprili, J. Gabelli, and J. Estève, Observation of the unconventional photon blockade in the microwave domain, Phys. Rev. Lett. **121**, 043602 (2018).

[133] H. J. Snijders, J. A. Frey, J. Norman, H. Flayac, V. Savona, A. C. Gossard, J. E. Bowers, M. P. van Exter, D. Bouwmeester, and W. Löffler, Observation of the unconventional photon blockade, Phys. Rev. Lett. **121**, 043601 (2018).

[134] F. Caruso, V. Giovannetti, C. Lupo, and S. Mancini, Quantum channels and memory effects, Rev. Mod. Phys. **86**, 1203 (2014).

[135] C. W. Gardiner and P. Zoller, *Quantum Noise* (Springer-Verlag, Berlin, 2000).

[136] H. P. Breuer and F. Petruccione, *The Theory of Open Quantum Systems* (Oxford University, New York, 2002).

[137] B. Vacchini and H. P. Breuer, Exact master equations for the non-Markovian decay of a qubit, Phys. Rev. A **81**, 042103 (2010).

[138] J. G. Li, J. Zou, and B. Shao, Non-Markovianity of the damped Jaynes-Cummings model with detuning, Phys. Rev. A **81**, 062124 (2010).

[139] H. Z. Shen, M. Qin, and X. X. Yi, Single-photon storing in coupled non-Markovian atom-cavity system, Phys. Rev. A **88**, 033835 (2013); R. Lo Franco, B. Bellomo, S. Maniscalco, and G. Compagno, Dynamics of quantum correlations in two-qubit systems within non-Markovian environments, Int. J. Mod. Phys. B **27**, 1345053 (2013).

[140] H. P. Breuer, D. Burgarth, and F. Petruccione, Non-Markovian dynamics in a spin star system: Exact solution and approximation techniques, Phys. Rev. B **70**, 045323 (2004); J. L. Li, H. Z. Shen, and X. X. Yi, Quantum batteries in non-Markovian reservoirs, Opt. Lett. **47**, 5614 (2022).

[141] E. Ferraro, M. Scala, R. Migliore, and A. Napoli, Non-Markovian dissipative dynamics of two coupled qubits in independent reservoirs: Comparison between exact solutions and master-equation approaches, Phys. Rev. A **80**, 042112 (2009); H. Z. Shen, S. Xu, Y. H. Zhou, and X. X. Yi, System susceptibility and bound-states in structured reservoirs, Opt. Express **27**, 31504 (2019).

[142] Z. Y. Xu, W. L. Yang, and M. Feng, Proposed method for direct measurement of the non-Markovian character of the qubits coupled to bosonic reservoirs, Phys. Rev. A **81**, 044105 (2010); H. Z. Shen, S. Xu, H. Li, S. L. Wu, and X. X. Yi, Linear response theory for periodically driven systems with non-Markovian effects, Opt. Lett. **43**, 2852 (2018).

[143] Z. He, J. Zou, L. Li, and B. Shao, Effective method of calculating the non-Markovianity N for single-channel open systems, Phys. Rev. A **83**, 012108 (2011).

[144] U. Weiss, *Quantum Dissipative Systems*, 4th ed. (World Scientific, Singapore, 2012).

[145] M. A. Nielsen and I. L. Chuang, *Quantum Computation and Quantum Information* (Cambridge University, Cambridge, England, 2000).

[146] T. D. Ladd, F. Jelezko, R. Laflamme, Y. Nakamura, C. Monroe, and J. L. O'Brien, Quantum computers, Nature (London) **464**, 45 (2010).

[147] L. Diósi, Non-Markovian open quantum systems: Input-output fields, memory, and monitoring, Phys. Rev. A **85**, 034101 (2012).

[148] J. Zhang, Y. X. Liu, R. B. Wu, K. Jacobs, and F. Nori, Non-Markovian quantum input-output networks, Phys. Rev. A **87**, 032117 (2013).

[149] G. M. Reuther, P. Hänggi, and S. Kohler, Non-Markovian qubit decoherence during dispersive readout, Phys. Rev. A **85**, 062123 (2012).

[150] V. Link, K. Müller, R. G. Lena, K. Luoma, F. Damanet, W. T. Strunz, and A. J. Daley, Non-Markovian quantum dynamics in strongly coupled multimode cavities conditioned on continuous measurement, PRX Quantum **3**, 020348 (2022).

[151] A. Burgess and M. Florescu, Non-Markovian dynamics of a single excitation within many-body dissipative systems, Phys. Rev. A **105**, 062207 (2022).

[152] U. Hoeppe, C. Wolff, J. Küchenmeister, J. Niegemann, M. Drescher, H. Benner, and K. Busch, Direct observation of non-Markovian radiation dynamics in 3D bulk photonic crystals, Phys. Rev. Lett. **108**, 043603 (2012).

[153] J. I. Costa-Filho, R. B. B. Lima, R. R. Paiva, P. M. Soares, W. A. M. Morgado, R. Lo Franco, and D. O. Soares-Pinto, Enabling quantum non-Markovian dynamics by injection of classical colored noise, Phys. Rev. A **95**, 052126 (2017).

[154] K. W. Chang and C. K. Law, Non-Markovian master equation for a damped oscillator with time-varying parameters, Phys. Rev. A **81**, 052105 (2010).

[155] S. Longhi, Non-Markovian decay and lasing condition in an optical microcavity coupled to a structured reservoir, Phys. Rev. A **74**, 063826 (2006).

[156] I. de Vega and D. Alonso, Dynamics of non-Markovian open quantum systems, Rev. Mod. Phys. **89**, 015001 (2017).

[157] H. T. Tan and W. M. Zhang, Non-Markovian dynamics of an open quantum system with initial system-reservoir correlations: A nanocavity coupled to a coupled-resonator optical waveguide, Phys. Rev. A **83**, 032102 (2011).

[158] S. Gröblacher, A. Trubarov, N. Prigge, G. D. Cole, M. Aspelmeyer, and J. Eisert, Observation of non-Markovian micromechanical Brownian motion, Nat. Commun. **6**, 7606 (2015).

[159] B. H. Liu, L. Li, Y. F. Huang, C. F. Li, G. C. Guo, E. M. Laine, H. P. Breuer, and J. Piilo, Experimental control of the transition from Markovian to non-Markovian dynamics of open quantum systems, Nat. Phys. **7**, 931 (2011).

[160] F. F. Fanchini, G. Karpat, B. Çakmak, L. K. Castelano, G. H. Aguilar, O. Jiménez Farías, S. P. Walborn, P. H. Souto Ribeiro, and M. C. de Oliveira, Non-Markovianity through accessible information, Phys. Rev. Lett. **112**, 210402 (2014).

[161] S. Haseli, G. Karpat, S. Salimi, A. S. Khorashad, F. F. Fanchini, B. Çakmak, G. H. Aguilar, S. P. Walborn, and P. H. Souto Ribeiro, Non-Markovianity through flow of information between a system and an environment, Phys. Rev. A **90**, 052118 (2014).

[162] S. J. Xiong, Q. W. Hu, Z. Sun, L. Yu, Q. P. Su, J. M. Liu, and C. P. Yang, Non-Markovianity in experimentally simulated quantum channels: Role of counterrotating-wave terms, Phys. Rev. A **100**, 032101 (2019).

[163] S. Cialdi, C. Benedetti, D. Tamascelli, S. Olivares, M. G. A. Paris, and B. Vacchini, Experimental investigation of the effect of classical noise on quantum non-Markovian dynamics, Phys. Rev. A **100**, 052104 (2019).

[164] D. Khurana, B. K. Agarwalla, and T. S. Mahesh, Experimental emulation of quantum non-Markovian dynamics and coherence protection in the presence of information backflow, Phys. Rev. A **99**, 022107 (2019).

[165] K. H. Madsen, S. Ates, T. Lund-Hansen, A. Löffler, S. Reitzenstein, A. Forchel, and P. Lodahl, Observation of Non-Markovian dynamics of a single quantum dot in a micropillar cavity, Phys. Rev. Lett. **106**, 233601 (2011).

[166] Y. Guo, P. Taranto, B. H. Liu, X. M. Hu, Y. F. Huang, C. F. Li, and G. C. Guo, Experimental demonstration of instrument-specific quantum memory effects and non-Markovian process recovery for common-cause processes, Phys. Rev. Lett. **126**, 230401 (2021).

[167] B. W. Li, Q. X. Mei, Y. K. Wu, M. L. Cai, Y. Wang, L. Yao, Z. C. Zhou, and L. M. Duan, Observation of Non-Markovian spin dynamics in a Jaynes-Cummings-Hubbard model using a trapped-ion quantum simulator, Phys. Rev. Lett. **129**, 140501 (2022).

[168] J. S. Xu, C. F. Li, C. J. Zhang, X. Y. Xu, Y. S. Zhang, and G. C. Guo, Experimental investigation of the non-Markovian dynamics of classical and quantum correlations, Phys. Rev. A **82**, 042328 (2010).

[169] J. S. Tang, C. F. Li, Y. L. Li, X. B. Zou, G. C. Guo, H. P. Breuer, E. M. Laine, and J. Piilo, Measuring non-Markovianity of processes with controllable system-environment interaction, Europhys. Lett. **97**, 10002 (2012).

[170] S. A. Uriri, F. Wudarski, I. Sinayskiy, F. Petruccione, and M. S. Tame, Experimental investigation of Markovian and non-Markovian channel addition, Phys. Rev. A **101**, 052107 (2020).

[171] M. H. Anderson, G. Vemuri, J. Cooper, P. Zoller, and S. J. Smith, Experimental study of absorption and gain by two-level atoms in a time-delayed non-Markovian optical field, Phys. Rev. A **47**, 3202 (1993).

[172] Z. D. Liu, Y. N. Sun, B. H. Liu, C. F. Li, G. C. Guo, S. Hamedani Raja, H. Lyyra, and J. Piilo, Experimental realization of high-fidelity teleportation via a non-Markovian open quantum system, Phys. Rev. A **102**, 062208 (2020).

[173] K. Goswami, C. Giarmatzi, C. Monterola, S. Shrapnel, J. Romero, and F. Costa, Experimental characterization of a non-Markovian quantum process, Phys. Rev. A **104**, 022432 (2021).

[174] M. Debiossac, M. L. Rosinberg, E. Lutz, and N. Kiesel, Non-Markovian feedback control and acausality: An experimental study, Phys. Rev. Lett. **128**, 200601 (2022).

[175] B. Bylicka, D. Chruściński, and S. Maniscalco, Non-Markovianity and reservoir memory of quantum channels: a quantum information theory perspective, Sci. Rep. **4**, 5720 (2014).

[176] S. B. Xue, R. B. Wu, W. M. Zhang, J. Zhang, C. W. Li, and T. J. Tarn, Decoherence suppression via non-Markovian coherent feedback control, Phys. Rev. A **86**, 052304 (2012).

[177] S. C. Hou, X. X. Yi, S. X. Yu, and C. H. Oh, Alternative non-Markovianity measure by divisibility of dynamical maps, Phys. Rev. A **83**, 062115 (2011).

[178] S. C. Hou, X. X. Yi, S. X. Yu, and C. H. Oh, Singularity of dynamical maps, Phys. Rev. A **86**, 012101 (2012).

[179] S. Lorenzo, F. Plastina, and M. Paternostro, Geometrical characterization of non-Markovianity, Phys. Rev. A **88**, 020102(R) (2013).

[180] Á. Rivas, S. F. Huelga, and M. B. Plenio, Entanglement and non-Markovianity of quantum evolutions, Phys. Rev. Lett. **105**, 050403 (2010).

[181] S. L. Luo, S. S. Fu, and H. T. Song, Quantifying non-Markovianity via correlations, Phys. Rev. A **86**, 044101 (2012).

[182] M. M. Wolf, J. Eisert, T. S. Cubitt, and J. I. Cirac, Assessing Non-Markovian quantum dynamics, Phys. Rev. Lett. **101**, 150402 (2008).

[183] X. M. Lu, X. G. Wang, and C. P. Sun, Quantum Fisher information flow and non-Markovian processes of open systems, Phys. Rev. A **82**, 042103 (2010).

[184] D. Chruściński and S. Maniscalco, Degree of non-Markovianity of quantum evolution, Phys. Rev. Lett. **112**, 120404 (2014).

[185] H. P. Breuer, E. M. Laine, J. Piilo, and B. Vacchini, Colloquium: Non-Markovian dynamics in open quantum systems, Rev. Mod. Phys. **88**, 021002 (2016).

[186] H. P. Breuer, E. M. Laine, and J. Piilo, Measure for the degree of non-Markovian behavior of quantum processes in open systems, Phys. Rev. Lett. **103**, 210401 (2009).

[187] E. M. Laine, J. Piilo, and H. P. Breuer, Measure for the non-Markovianity of quantum processes, Phys. Rev. A **81**, 062115 (2010).

[188] C. Addis, B. Bylicka, D. Chruściński, and S. Maniscalco, Comparative study of non-Markovianity measures in exactly solvable one- and two-qubit models, Phys. Rev. A **90**, 052103 (2014).

[189] S. Wißmann, A. Karlsson, E. M. Laine, J. Piilo, and H. P. Breuer, Optimal state pairs for non-Markovian quantum dynamics, Phys. Rev. A **86**, 062108 (2012).

[190] S. Wißmann, H. P. Breuer, and B. Vacchini, Generalized trace-distance measure connecting quantum and classical non-Markovianity, Phys. Rev. A **92**, 042108 (2015).

[191] N. Bartolo, F. Minganti, W. Casteels, and C. Ciuti, Exact steady state of a Kerr resonator with one- and two-photon driving and dissipation: Controllable Wigner-function multimodality and dissipative phase transitions, Phys. Rev. A **94**, 033841 (2016).

[192] F. Minganti, N. Bartolo, J. Lolli, W. Casteels, and C. Ciuti, Exact results for Schrödinger cats in driven-dissipative systems and their feedback control, Sci. Rep. **6**, 26987 (2016).

[193] S. T. Shen, Y. Qu, J. H. Li, and Y. Wu, Tunable photon statistics in parametrically amplified photonic molecules, Phys. Rev. A **100**, 023814 (2019)

[194] P. D. Nation, J. R. Johansson, M. P. Blencowe, and F. Nori, Colloquium: Stimulating uncertainty: Amplifying the quantum vacuum with superconducting circuits, Rev. Mod. Phys. **84**, 1 (2012).

[195] Z. Leghtas, S. Touzard, I. M. Pop, A. Kou, B. Vlastakis, A. Petrenko, K. M. Sliwa, A. Narla, S. Shankar, M. J. Hatridge, M. Reagor, L. Frunzio, R. J. Schoelkopf, M. Mirrahimi, and M. H. Devoret, Confining the state of light to a quantum manifold by engineered two-photon loss, Science **347**, 853 (2015).

[196] A. F. Adiyatullin, M. D. Anderson, H. Flayac, M. T. Portella-Oberli, F. Jabeen, C. Ouellet-Plamondon, G. C. Sallen, and B. Deveaud, Periodic squeezing in a polariton Josephson junction, Nat. Commun. **8**, 1329 (2017).

[197] A. A. Clerk, M. H. Devoret, S. M. Girvin, F. Marquardt, and R. J. Schoelkopf, Introduction to quantum noise, measurement, and amplification, Rev. Mod. Phys. **82**, 1155 (2010).

[198] R. W. Boyd, *Nonlinear Optics*, 3rd ed. (Academic, New York, 2008).

[199] T. C. H. Liew and Y. G. Rubo, Quantum exciton-polariton networks through inverse four-wave mixing, Phys. Rev. B **97**, 041302(R) (2018).

[200] D. Stefanatos and E. Paspalakis, Boosting entanglement between exciton-polaritons with on-off switching of Josephson coupling, Phys. Rev. B **98**, 035303 (2018).

[201] L. Mazzola, S. Maniscalco, J. Piilo, K. A. Suominen, and B. M. Garraway, Pseudomodes as an effective description of memory: Non-Markovian dynamics of two-state systems in structured reservoirs, Phys. Rev. A **80**, 012104 (2009).

[202] G. Pleasance and B. M. Garraway, Application of quantum Darwinism to a structured environment, Phys. Rev. A **96**, 062105 (2017).

[203] M. W. Jack and J. J. Hope, Resonance fluorescence in a band-gap material: Direct numerical simulation of non-Markovian evolution, Phys. Rev. A **63**, 043803 (2001).

[204] S. M. Barnett and P. M. Radmore, *Methods in Theoretical Quantum Optics* (Oxford University, New York, 2002).

[205] B. M. Garraway, Nonperturbative decay of an atomic system in a cavity, Phys. Rev. A **55**, 2290 (1997).

[206] B. M. Garraway, Decay of an atom coupled strongly to a reservoir, Phys. Rev. A **55**, 4636 (1997).

[207] D. Tamascelli, A. Smirne, S. F. Huelga, and M. B. Plenio, Nonperturbative treatment of non-Markovian dynamics of open quantum systems, Phys. Rev. Lett. **120**, 030402 (2018).

[208] B. J. Dalton, S. M. Barnett, and B. M. Garraway, Theory of pseudomodes in quantum optical processes, Phys. Rev. A **64**, 053813 (2001).

[209] L. Mazzola, S. Maniscalco, J. Piilo, K. A. Suominen, and B. M. Garraway, Sudden death and sudden birth of entanglement in common structured reservoirs, Phys. Rev. A **79**, 042302 (2009).

[210] C. Lazarou, K. Luoma, S. Maniscalco, J. Piilo, and B. M. Garraway, Entanglement trapping in a nonstationary structured reservoir, Phys. Rev. A **86**, 012331 (2012).

[211] Z. X. Man, N. B. An, and Y. J. Xia, Non-Markovianity of a two-level system transversally coupled to multiple bosonic reservoirs, Phys. Rev. A **90**, 062104 (2014).

[212] Z. X. Man, N. B. An, and Y. J. Xia, Non-Markovian dynamics of a two-level system in the presence of hierarchical environments, Opt. Express **23**, 5763 (2015).

[213] D. W. Schönleber, A. Croy, and A. Eisfeld, Pseudomodes and the corresponding transformation of the temperature-dependent bath correlation function, Phys. Rev. A **91**, 052108 (2015).

[214] D. Aghamalyan, J. B. You, H. S. Chu, C. E. Png, L. Krivitsky, and L. C. Kwek, Tunable quantum switch realized with a single Λ-level atom coupled to the microtoroidal cavity, Phys. Rev. A **100**, 053851 (2019).

[215] T. K. Mavrogordatos and J. Larson, Monitoring the resonantly driven Jaynes-Cummings oscillator by an external two-level emitter: A cascaded open-systems approach, Phys. Rev. A **101**, 053849 (2020).

[216] T. K. Mavrogordatos, Collective atomic correlations in absorptive optical bistability without adiabatic elimination: Exemplifying nonclassicality from a linearized treatment of fluctuations, Phys. Rev. A **102**, 053708 (2020).

[217] L. S. Bishop, E. Ginossar, and S. M. Girvin, Response of the strongly driven Jaynes-Cummings oscillator, Phys. Rev. Lett. **105**, 100505 (2010).

[218] U. B. Hoff, J. Kollath-Bönig, J. S. Neergaard-Nielsen, and U. L. Andersen, Measurement-induced macroscopic superposition states in cavity optomechanics, Phys. Rev. Lett. **117**, 143601 (2016).

[219] A. Kubanek, A. Ourjoumtsev, I. Schuster, M. Koch, P. W. H. Pinkse, K. Murr, and G. Rempe, Two-photon gateway in one-atom cavity quantum electrodynamics, Phys. Rev. Lett. **101**, 203602 (2008).

[220] V. Link and W. T. Strunz, Dynamical phase transitions in dissipative quantum dynamics with quantum optical realization, Phys. Rev. Lett. **125**, 143602 (2020).

[221] B. L. Hu, J. P. Paz, and Y. H. Zhang, Quantum Brownian motion in a general environment: Exact master equation with nonlocal dissipation and colored noise, Phys. Rev. D **45**, 2843 (1992).

[222] J. J. Halliwell and T. Yu, Alternative derivation of the Hu-Paz-Zhang master equation of quantum Brownian motion, Phys. Rev. D **53**, 2012 (1996).

[223] G. W. Ford and R. F. O'Connell, Exact solution of the Hu-Paz-Zhang master equation, Phys. Rev. D **64**, 105020 (2001).

[224] C. P. Sun and L. H. Yu, Exact dynamics of a quantum dissipative system in a constant external field, Phys. Rev. A **51**, 1845 (1995).

[225] C. P. Sun, Y. B. Gao, H. F. Dong, and S. R. Zhao, Partial factorization of wave functions for a quantum dissipative system, Phys. Rev. E **57**, 3900 (1998).

[226] L. H. Yu and C. P. Sun, Evolution of the wave function in a dissipative system, Phys. Rev. A **49**, 592 (1994).

[227] C. H. Chou, T. Yu, and B. L. Hu, Exact master equation and quantum decoherence of two coupled harmonic oscillators in a general environment, Phys. Rev. E **77**, 011112 (2008).

[228] R. Karrlein and H. Grabert, Exact time evolution and master equations for the damped harmonic oscillator, Phys. Rev. E **55**, 153 (1997); H. Z. Shen, D. X. Li, S. L. Su, Y. H. Zhou, and X. X. Yi, Exact non-Markovian dynamics of qubits coupled to two interacting environments, Phys. Rev. A **96**, 033805 (2017).

[229] A. Pereverzev, Damped harmonic oscillator: Pure states of the bath and exact master equations, Phys. Rev. E **68**, 026111 (2003).

[230] W. M. Zhang, P. Y. Lo, H. N. Xiong, M. W. Y. Tu, and F. Nori, General non-Markovian dynamics of open quantum systems, Phys. Rev. Lett. **109**, 170402 (2012).

[231] H. Z. Shen, S. L. Su, Y. H. Zhou, and X. X. Yi, Non-Markovian quantum Brownian motion in one dimension in electric fields, Phys. Rev. A **97**, 042121 (2018).

[232] S. Ferretti and D. Gerace, Single-photon nonlinear optics with Kerr-type nanostructured materials, Phys. Rev. B **85**, 033303 (2012).

[233] H. Z. Shen, S. Xu, H. T. Cui, and X. X. Yi, Non-Markovian dynamics of a system of two-level atoms coupled to a structured environment, Phys. Rev. A **99**, 032101 (2019); H. Z. Shen, H. Li, Y. F. Peng, and X. X. Yi, Mechanism for Hall conductance of two-band systems against decoherence, Phys. Rev. E **95**, 042129 (2017).

[234] H. Z. Shen, S. Xu, S. Yi, and X. X. Yi, Controllable dissipation of a qubit coupled to an engineering reservoir, Phys. Rev. A **98**, 062106 (2018); H. Z. Shen, X. Q. Shao, G. C. Wang, X. L. Zhao, and X. X. Yi, Quantum phase transition in a coupled two-level system embedded in anisotropic three-dimensional photonic crystals, Phys. Rev. E **93**, 012107 (2016); Q.-J. Tong, J.-H. An, H.-G. Luo, and C.-H. Oh, Mechanism of entanglement preservation, Phys. Rev. A **81**, 052330 (2010); S.-Y. Bai and J.-H. An, Floquet engineering to overcome no-go theorem of noisy quantum metrology, Phys. Rev. Lett. **131**, 050801 (2023).

[235] T. Shi, Y. H. Wu, A. González-Tudela, and J. I. Cirac, Bound states in boson impurity models, Phys. Rev. X **6**, 021027 (2016); Z. Y. Li and H. Z. Shen, Non-Markovian dynamics with a giant atom coupled to a semi-infinite photonic waveguide, Phys. Rev. A **109**, 023712 (2024); Q. J. Tong, J. H. An, H. G. Luo, and C. H. Oh, Quantum phase transition in the delocalized regime of the spin-boson model, Phys. Rev. B **84**, 174301 (2011); W. L. Song, H. B. Liu, B. Zhou, W. L. Yang, and J. H. An, Remote charging and degradation suppression for the quantum battery, Phys. Rev. Lett. **132**, 090401 (2024).

[236] H. Z. Shen, Y. Chen, T. Z. Luan, and X. X. Yi, Multiple single-photon generations in three-level atoms coupled to cavity with non-Markovian effects, Phys. Rev. A **107**, 053705 (2023); T. Shi, Y. H. Wu, A. González-Tudela, and J. I. Cirac, Effective many-body Hamiltonians of qubit-photon bound states, New J. Phys. **20**, 105005 (2018).

[237] L. Xin, S. Xu, X. X. Yi, and H. Z. Shen, Tunable non-Markovian dynamics with a three-level atom mediated by the classical laser in a semi-infinite photonic waveguide, Phys. Rev. A **105**, 053706 (2022); G. Calajó and P. Rabl, Strong coupling between moving atoms and slow-light Cherenkov photons, *ibid.* **95**, 043824 (2017).

[238] T. Shi, Y. Chang, and J. J. García-Ripoll, Ultrastrong coupling few-photon scattering theory, Phys. Rev. Lett. **120**, 153602 (2018); H. Z. Shen, Q. Wang, and X. X. Yi, Dispersive readout with non-Markovian environments, Phys. Rev. A **105**, 023707 (2022).

[239] L. Lo and C. K. Law, Quantum radiation from a shaken two-level atom in vacuum, Phys. Rev. A **98**, 063807 (2018).

[240] W. Zhang and H. Z. Shen, Optomechanical second-order sidebands and group delays in a spinning resonator with a parametric amplifier and non-Markovian effects, Phys. Rev. A **109**, 033701 (2024); W. Z. Zhang, J. Cheng, W. D. Li, and L. Zhou, Optomechanical cooling in the non-Markovian regime, *ibid.* **93**, 063853 (2016).

[241] W. Z. Zhang, Y. Han, B. Xiong, and L. Zhou, Optomechanical force sensor in a non-Markovian regime, New J. Phys. **19**, 083022 (2017).

[242] J. F. Triana, A. F. Estrada, and L. A. Pachón, Ultrafast optimal sideband cooling under non-Markovian evolution, Phys. Rev. Lett. **116**, 183602 (2016).

[243] J. C. Sankey, C. Yang, B. M. Zwickl, A. M. Jayich, and J. G. E. Harris, Strong and tunable nonlinear optomechanical coupling in a low-loss system, Nat. Phys. **6**, 707 (2010).

[244] M. Bhattacharya, H. Uys, and P. Meystre, Optomechanical trapping and cooling of partially reflective mirrors, Phys. Rev. A **77**, 033819 (2008).

[245] H. K. Cheung and C. K. Law, Nonadiabatic optomechanical Hamiltonian of a moving dielectric membrane in a cavity, Phys. Rev. A **84**, 023812 (2011).

[246] M. Aspelmeyer, T. J. Kippenberg, and F. Marquardt, Cavity optomechanics, Rev. Mod. Phys. **86**, 1391 (2014).

[247] J. D. Thompson, B. M. Zwickl, A. M. Jayich, F. Marquardt, S. M. Girvin, and J. G. E. Harris, Strong dispersive coupling of a high-finesse cavity to a micromechanical membrane, Nature (London) **452**, 72 (2008).

[248] B. Coutinho dos Santos, K. Dechoum, A. Z. Khoury, L. F. da Silva, and M. K. Olsen, Quantum analysis of the nondegen-

erate optical parametric oscillator with injected signal, Phys. Rev. A **72**, 033820 (2005).

[249] D. F. Walls and G. J. Milburn, *Quantum Optics* (Springer-Verlag, Berlin, 1994).

[250] C. C. Gerry and P. L. Knight, *Introductory Quantum Optics* (Cambridge University, Cambridge, England, 2005).

[251] W. Qin, A. Miranowicz, P. B. Li, X. Y. Lü, J. Q. You, and F. Nori, Exponentially enhanced light-matter interaction, cooperativities, and steady-state entanglement using parametric amplification, Phys. Rev. Lett. **120**, 093601 (2018); C. Shang and H. C. Li, Resonance-dominant optomechanical entanglement in open quantum systems, arXiv:2307.12383.

[252] C. W. Gardiner and M. J. Collett, Input and output in damped quantum systems: Quantum stochastic differential equations and the master equation, Phys. Rev. A **31**, 3761 (1985).

[253] S. M. Barnett and P. M. Radmore, *Methods in Theoretical Quantum Optics* (Clarendon, Oxford, 1997).